J. Physiol. (1959) 145, 289–325

TRANSMISSION AT THE GIANT MOTOR SYNAPSES OF THE CRAYFISH

By E. J. FURSHPAN* and D. D. POTTER*

From the Biophysics Department, University College London

(*Received* 30 *July* 1958)

A number of studies have recently been made on the mechanism of impulse transmission across (*a*) the neuromuscular junction (del Castillo & Katz, 1956), (*b*) certain synapses on the motoneurone (Eccles, 1957) and (*c*) the nerve–electroplaque junction (Grundfest, 1957). In each case it seems likely that local circuit action stops at the junction and that the prejunctional action currents contribute very little to the observed post-synaptic potentials. At all these synapses, however, the prejunctional terminals are too small to be impaled with micro-electrodes and it has not been possible to determine quantitatively the resistance of the junction to local current flow (see, however, del Castillo & Katz, 1954). Therefore it seemed of interest to study a synapse in which both elements were amenable to the use of intracellular electrodes. Several such junctions, with large pre- and post-synaptic units, are known in invertebrate nervous systems (Johnson, 1924; Stough, 1926; Young, 1939). The particular ones chosen were the giant motor synapses (GMS's) of the abdominal nerve cord of the crayfish. The anatomy of the GMS's, which will be discussed in greater detail below, has been studied by Johnson (1924) with the light microscope and by Robertson (1952, 1953, 1955) with the electron microscope. Wiersma (1947) has recorded the electrical responses of the synaptic elements using extracellular electrodes. He found that in preparations in good condition, a single presynaptic impulse evoked one conducted post-synaptic spike and that transmission took place in only one direction.

One interesting aspect of the GMS's is that the 'pre-fibres' (presynaptic fibres) are even larger than the 'post-fibres' (post-synaptic fibres). The possibility was, therefore, considered from the beginning that the presynaptic action currents would stimulate the post-fibre, i.e. that an 'electrical' mechanism of transmission operated (Fatt, 1954). Strong evidence has been obtained to support this view. It has also been found that the 'synaptic

* U.S. Public Health Service Fellows. Present address: Wilmer Institute, The Johns Hopkins Medical School, Baltimore 5, Maryland, U.S.A.

membrane' has the properties of an electric rectifier, which explains the one-way character of the transmission. A preliminary account of this work has been published (Furshpan & Potter, 1957).

METHODS

The anatomy of the synaptic elements

The following description is based mainly on Johnson (1924).

Pre-fibres. Two pairs of giant axons constitute the pre-fibres of the crayfish GMS's. The medial pair extend unbranched and without interruption through almost the entire length of the nerve cord. Each member of the lateral pair, on the other hand, consists of a longitudinal chain of separate axons. The abdominal portion of a lateral giant axon is formed by six such axon segments, each joined to the next by a junction which will be referred to as a 'segmental' synapse.

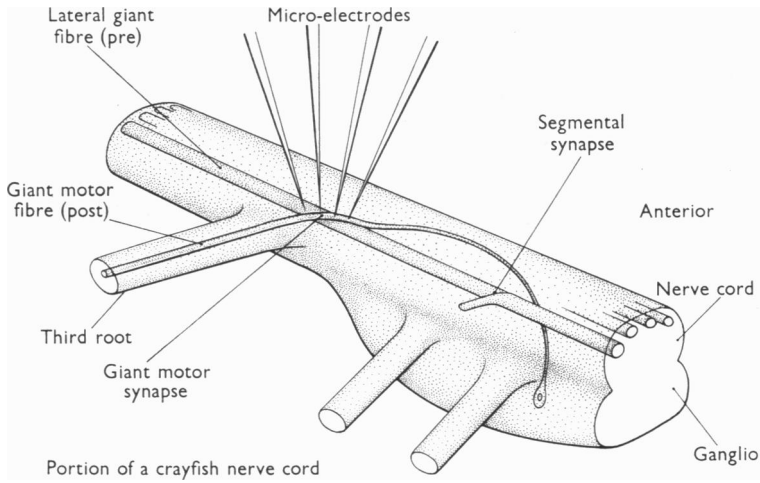

Text-fig. 1. Semidiagrammatic drawing of a portion of a crayfish abdominal nerve cord, containing one ganglion. The course of one motor giant axon is shown from its cell body in the ventral part of the ganglion (Hardy, 1894; Johnson, 1924) until it leaves the third ganglionic root on the opposite side of the cord. Only its junction with the lateral giant pre-fibre is shown; but its synapses with the two medial giant fibres are located just centrally, where the latter fibres cross the motor axon. A synapse between two segments of the lateral giant fibre is also shown. The ventral continuation of the anterior segment presumably goes to the cell body and also provides the collateral, which makes synaptic connexion with that of the contralateral segment (not shown).

Wiersma (1947) has shown that the nerve impulse crosses these junctions in either direction. In preliminary experiments using intracellular electrodes we have found that electrotonic currents flow freely across them in either direction (cf. Kao & Grundfest, 1956); but they seem to be regions of low safety factor at which spikes, in depressed preparations, may be blocked. Text-fig. 1 shows parts of two segments of a lateral giant axon with a synapse between them.

Post-fibres. The post-fibres are giant motor axons which innervate the flexor musculature of the tail (abdomen). There is one such fibre on each side of the first five abdominal ganglia, the sixth ganglion having two pairs. The cell body lies close to the ventral surface of the ganglion (Text-fig. 1). From there the axon extends dorsally, making synaptic connexion with a number of fibres before finally emerging from the cord in the third (ganglionic) root of the opposite side.

The motor giant axons will be designated by the side of the cord from which they emerge rather than the side on which the cell body lies. Histological evidence (Johnson, 1924; Wiersma, 1947) suggests that the motor giant axon forms synapses with the following fibres: (1) the ipsilateral segmental (lateral) giant axon, (2) the ipsilateral medial giant axon, (3) the contralateral medial giant axon, (4) the collateral (see Results, p. 297) of the contralateral segmental giant axon, and (5) the contralateral motor giant axon at the point at which both cross the mid line. Wiersma (1947) has shown that one-to-one transmission can occur at synapses (1), (2) and (3); but there is as yet no physiological evidence for the presence of synapses (4) and (5) (but see below, p. 303). In the experiments to be described synapse (1) has been used almost exclusively and it is the the only one shown in Text-fig. 1. Its structure is described in the Discussion (p. 319). The presence of yet other synapses on the giant motor fibre will be considered in the following paper (Furshpan & Potter, 1959).

Experimental procedure

The preparation. The crayfish *Astacus fluviatilis* was used in all experiments. The part of the nerve cord extending from the last thoracic ganglion to the last abdominal ganglion was dissected from the animal as follows. After removal of the dorsal parts of the thoracic and abdominal exoskeleton the animal was secured in a bath of saline, dorsal side up. The attachments of the third roots to the flexor muscles were exposed by dividing the musculature along the mid line. The third roots were then severed as far from the cord as possible and the muscles entirely removed. The first and second roots of each ganglion were cut at least 1 mm from the cord and then the cord itself was freed from the connective tissue binding it to the floor of the abdomen and thorax.

In order to reduce displacement of the cord during experimental manipulations, it was fixed to a platform in a Perspex perfusion chamber in the following way. The platform possessed two parallel-sided grooves (0·45 mm wide and 2·5 mm apart) between which the cord was placed with its longitudinal axis parallel to the grooves and its dorsal surface uppermost. The first and second roots of each ganglion, which were not otherwise used, were then wedged into the grooves on their respective sides with short lengths of 26 S.W.G. platinum wire.

Dark-field illumination considerably aided the observation of the synaptic elements and was used in all experiments. In order to allow the condenser to be brought sufficiently close to the preparation, an aperture was cut into the Perspex plate which supported the perfusion chamber. The condenser was raised and lowered with a rack and pinion device. It was convenient to be able to move the chamber, in the horizontal plane, with respect to the condenser and a mechanical stage was used to fix the chamber to the supporting plate.

In order to expose the axons for impaling, the sheath which encloses the cord was removed from the dorsal surface of the ganglion and of the region of cord immediately posterior to it. It was especially important to perform this operation with care to avoid serious injury to the synaptic elements.

Both pre- and post-fibres could be stimulated with external electrodes. In the case of the post-fibre the third root was carefully drawn into a glass capillary with the aid of a small hypodermic syringe. The stimulating voltage was then applied between the inside of the capillary and the bath. A similar method was used for the pre-fibre; but instead of drawing the axon into the capillary, the latter was placed on the surface of the cord over the axon. The slight negative pressure supplied by the syringe produced a partial sealing of the capillary to the fibre and reduced the shunting of the stimulating current.

Impaling the axons. The fibres forming the GMS lie very close to the dorsal surface of the cord, and after removal of the sheath they are accessible for the insertion of the micro-electrodes. With dark-field illumination the giant pre-fibres were almost always clearly visible as broad dark bands contrasting with the rest of the cord, which appeared bright. The giant motor fibre usually could not be clearly distinguished, but its position could almost always be inferred from slight visual clues and the fact that it is the most posterior of the large fibres entering the third root (see also Hardy, 1894). In any case, the criteria for accepting a successful entry into a motor giant axon were entirely physiological (see below, p. 298).

In spite of the large number of preparations which were made, each containing ten potentially usable giant motor synapses, the number of successful experiments has been relatively small. The chief impediment has been the difficulty experienced in the insertion of the micro-electrodes. It was usually easier to impale the lateral giant axons than the medial ones, and the former were used as pre-fibres in almost all experiments. The giant motor axons were usually the most difficult of the fibres to enter. The pre-fibre electrodes were inserted first, for once inside the cell they were not easily dislodged by further manipulation.

In some experiments two micro-electrodes were inserted into each fibre; in other experiments only one. When four electrodes were used, the two within a single fibre were separated from one another by 0·05–0·3 mm (usually about 0·15 mm). The distance from the nearest pre-fibre electrode to the edge of the post-fibre (at the synapse) was usually within the same range. At least one, and sometimes both, of the post-fibre electrodes were inserted in the region of fibre-crossing.

Before experience had been gained in locating the motor giant axon, entries were often made, inadvertently, into the smaller axons which also leave the cord in the third root (Pl. 1). These fibres cross over the lateral giant axon in the same general region as does the motor giant axon and there is physiological evidence that at least some of them make synaptic connexion with the lateral giant axon. The position of the junctions, however, does not seem to be at the place of crossing, but at some other site, probably deeper within the cord. The analysis of the GMS which is given below cannot be applied to these synapses, for such analysis requires either that the internal recording electrodes be close to the junction, or at least that their distance from the synapse, as well as the characteristic lengths of the junctional elements, be known. Text-fig. 2 shows the response recorded from one of the smaller third root fibres following stimulation of the lateral giant axon. The post-synaptic potential is much slower and the synaptic delay longer than in the case of a GMS (see Text-fig. 7*b* for comparison), but without knowing the position of the junction, little can be deduced about the mechanism of the transmission process. The prolonged time course and delay of the post-synaptic response might equally well be due to chemical transmitter action, to electrotonic decrement within the post-fibre or to a combination of both factors. It was, therefore, very important to know which of the third-root fibres the post-synaptic electrodes had entered, for only the giant motor axon is known to make a synapse with the lateral pre-fibre at the place of crossing it. The criteria used for recognizing an entry into a motor giant will be described below (see Results, p. 298).

Micro-electrodes. Especially in the case of post-fibres, only micro-pipettes with very fine tip diameters could be successfully inserted; but it was also necessary that the electrodes should pass relatively large currents. It was found that micropipettes of 15–20 MΩ resistance, pulled from Pyrex glass tubing with an outside diameter of about 2 mm and wall thickness about 0·35 mm, usually met the above specifications without being too fragile. Selection of the glass tubing for the appropriate wall thickness was done with the aid of a microscope and ocular micrometer.

The four micro-electrodes were held by separate micromanipulators and the tips of all electrodes could be manœuvred within the same small field. The usual techniques for intracellular potential recording and passing of current across fibre membranes were used (Fatt & Katz, 1951), except for the method of inserting the current-passing electrodes. Each micropipette could be used to pass current or to measure voltage and was used in the latter way to register resting potential during insertion. The probe unit of each of the four cathode-followers contained a pair of micro-switches operated simultaneously by a single lever. In one position of the switches, the Ag–AgCl wire from the micro-electrode was connected to the grid of the cathode-follower probe valve (see Text-fig. 3); and the metal shielding surrounding (*a*) the probe valve, (*b*) the Ag–AgCl wire, and (*c*) the upper part of the micro-electrode, was connected to the cathode of the same valve (Nastuk & Hodgkin, 1950). With the alternative switch position, the connexion of the Ag–AgCl wire was changed from the grid to a lead to the current generator and all the shielding associated with that channel was switched from cathode to earth. Also, when current was being passed, the grid of the reference valve of that cathode-follower was switched from the bath electrode to earth.

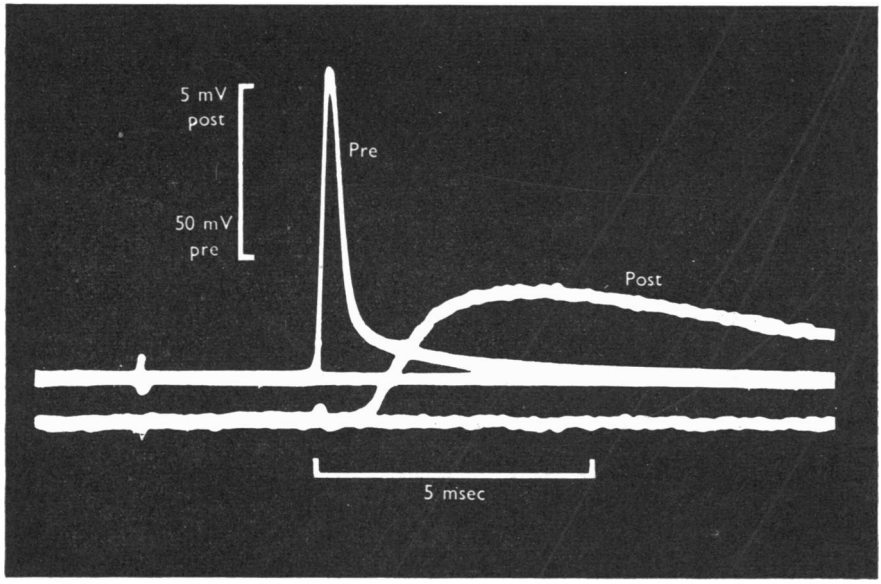

Text-fig. 2. The post-synaptic response, of one of the smaller fibres of the third root, to stimulation of the lateral giant axon of the same side. The pre-fibre spike is shown above, the p.s.p. below. Compare the delay and the time course of the p.s.p. with that of a giant motor synapse (Text-fig. 7). Intracellular recording in this and all subsequent records. Voltage calibration: 50 mV, pre-; 5 mV, post-.

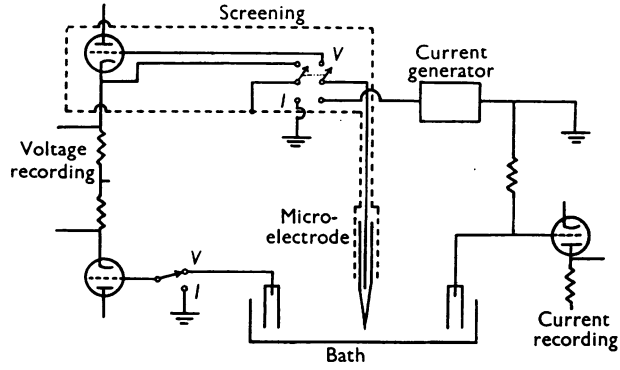

Text-fig. 3. The switching arrangement for alternatively passing current or recording potential with a micro-electrode. There are separate switches and cathode followers for each of the four micro-electrodes, but only one two-channel current generator. Leads from each switch are available, however, for plugging into either channel.

Switching the shielding and the reference-valve grid to earth when current was being passed decreased the capacitative artifact recorded in other channels. The potential across the current-monitoring resistance, as well as the output of any of the cathode-followers, could be led into either of two DC amplifiers, and observed on the screen of a double-beam oscilloscope.

For the experiments to be most useful it was necessary to collect a large amount of data. In order that the measurements could all be made within a short period of time, a recording method similar to that used by Cole & Curtis (1941) was found to be convenient. It is illustrated in Text-fig. 4, which shows the relationship of steady-state current to membrane potential for the lateral giant pre-fibre. The recording was made by switching the connexion of the X-plates of the cathode-ray tube from the time base generator to the second DC amplifier. Then the output of one amplifier moved the beam vertically, while the output of the other gave horizontal deflexions.

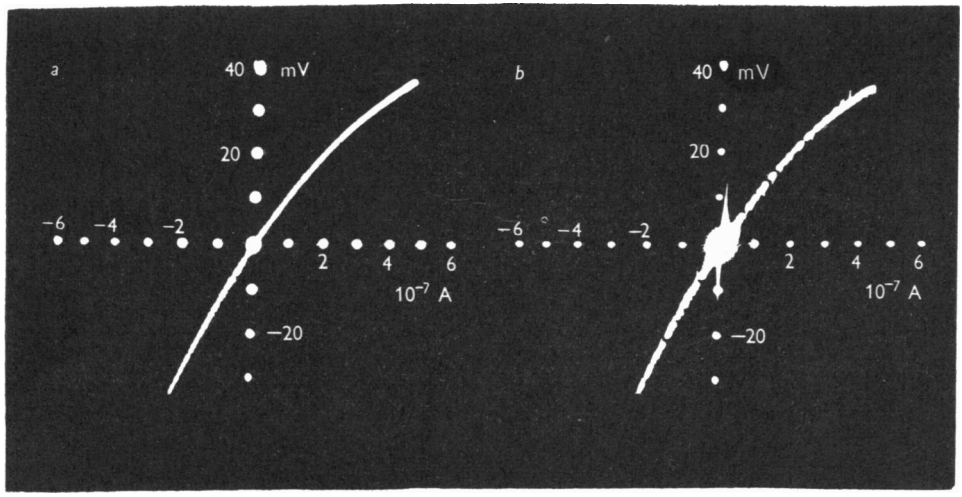

Text-fig. 4. The direct recording from the oscilloscope of current–voltage curves of a lateral giant axon. The potential across a monitor resistance, which was proportional to the current applied to the fibre through one micro-electrode, was registered on the abscissa; while the membrane potential of the fibre, recorded by a second nearby intracellular electrode, was recorded on the ordinate. In *a*, the current applied to the fibre was rapidly increased in small increments by manual operation of the wire-wound potentiometer controlling the DC output of the current generator. In *b* rectangular current pulses of varying sizes and 70 msec in duration were applied to the fibre, while recording current and voltage as in *a*. Each pulse produced one of the points on the curve. Records of this kind served as controls for those of the first type.

In Text-fig. 4*a* the applied current was recorded as a horizontal deflexion, while the concomitant changes in the membrane potential were registered as a vertical deflexion. The current, which was varied by manual operation of the output potentiometer of the current generator, was steadily increased during a period of 1–2 sec. It was also possible to pass rectangular (70 msec) pulses of current of various magnitudes. Then a number of points were obtained lying along the same curve as is shown in Text-fig. 4*b*. Both types of record were usually made, the second serving as a control for the first; for there was some question whether the rate of increase of current during manual control of the potentiometer would affect the slope of the current–voltage curve. The error attributable to this factor was usually found to be negligible and it was then preferable to

use the first type of record (Text-fig. 4*a*), which allowed more accurate determination of the origin. The points which give the axes in Text-fig. 4 were produced with a decade calibrator. The photographic record, then, is a multiple exposure of calibrating voltage steps of both polarities applied to both channels and the current–voltage relationship of the fibre membrane for both a inward and outward currents. Less than a minute was usually required to complete such record.

When studying the properties of the GMS with only two micro-electrodes, the graphs made were similar, but related membrane potential of one fibre to the current applied to the other. The experiments which gave the most information, however, were those in which two electrodes were inserted into each axon. In these cases the membrane potentials of both fibres were simultaneously recorded on rectangular co-ordinates, while using the remaining internal electrodes to apply current first to one axon and then the other.

The physiological saline was made according to the formula of van Harreveld (1936) and had the following composition: (mM) NaCl 205, $CaCl_2$ 13·5, KCl 5·4, $MgCl_2$ 2·6, $NaHCO_3$ 2·3. Experiments were usually made at about 20° C.

Histology. In order to estimate the diameter of the presynaptic and post-synaptic axons and the area of synaptic contact, histological preparations were made from the nerve cords of five crayfish. The cords were fixed for a few hours in cold vom Rath's fixative (vom Rath, 1895) to which $CaCl_2$ had been added to a final concentration of 1%. It was found that the outside dimensions of the cords were decreased by about 20% during the histological preparation and the measurements of axon diameter were increased in the same proportion. The diameters of the lateral, medial and motor giant axons were variable along the course of the fibres, even within a single segment. It is possible that, in the case of the pre-fibres, this variation was largely an artifact of histological preparation. The diameter of the lateral giant axons was found to be $91{\cdot}7 \pm 3{\cdot}0\mu$ (mean ± S.E.), that of the medial giant axons, $59{\cdot}1 \pm 2{\cdot}8\mu$. The motor axons showed a more or less abrupt increase in diameter, about twofold or more, at the point at which they crossed the mid line and formed synapses with the motor fibre of the opposite side. They usually reached their largest diameter while passing under the ipsilateral medial giant axon, and then gradually became thinner as they crossed over the lateral pre-fibre. The diameter of the motor axons at the point at which they formed synapses with the lateral fibres was $38{\cdot}5 \pm 1{\cdot}6\mu$. All the above diameters are the means of about twenty measurements from seven different ganglia.

Synaptic contact between the two axons comes about by means of numerous processes of the post-fibre which penetrate intervening sheaths and come into close association with pre-fibre membrane (Robertson, 1953, 1955; see Discussion). In several of our preparations it was possible to see that these post-fibre processes expanded before terminating, thus providing an enlarged area of contact between the two membranes. In one of these cords the terminal expansions could be seen sufficiently clearly to be measured in serial sections and thus an estimate of the total area of synaptic contact could be made. The value found was 6×10^{-5} cm², with a range of uncertainty of $3\text{–}8 \times 10^{-5}$ cm². This cord, which was not used for measuring axon diameters, was taken from a smaller animal than were those on which the electrical recordings were made; and in calculating the resistance of a unit area of the 'synaptic membrane' (see Discussion) a value of 10^{-4} cm² was used.

RESULTS

Identification of the impaled axons

Lateral giant pre-fibres. With few exceptions the micro-electrode could be placed into the lateral giant axon at the first attempt. Examples of the action potentials of these fibres are shown in Text-fig. 5. The largest part of the falling phase was complete in 1–1·5 msec after the start of the spike and was followed by a more prolonged 'tail'. The small deflexion several milliseconds after the spike, in *a* (indicated by the arrow), was observed in a number of preparations

and was found to coincide with the firing of the lateral giant segment on the opposite side of the cord. Text-fig. 5*c* shows simultaneous intracellular recordings from the right and left lateral giant axons, at the same level of the cord. The right segment was stimulated by means of a third internal electrode and the resulting spike arose from the local electrotonic pulse. Accompanying this

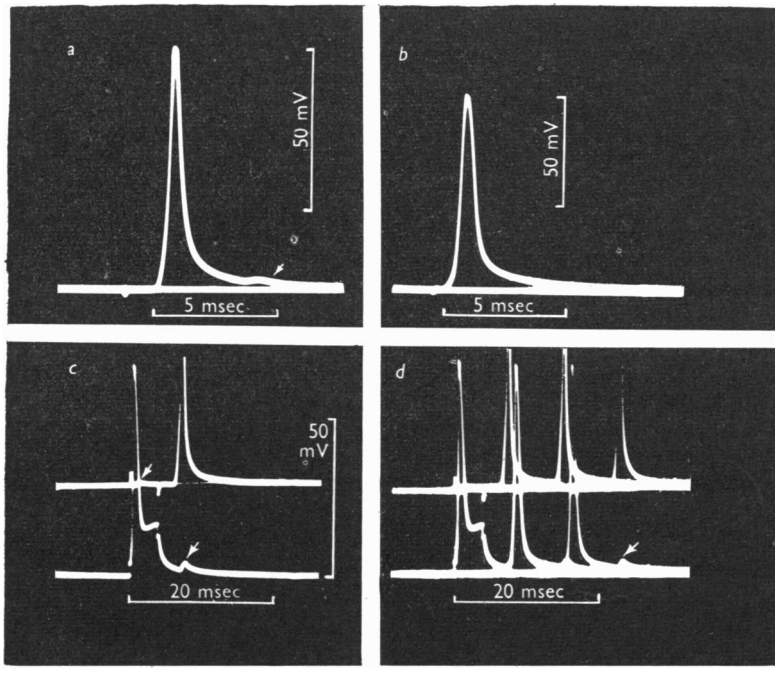

Text-fig. 5. Action potentials recorded intracellularly from lateral giant pre-fibres. Stimulation in *a* and *b* was through external, and in *c* and *d* internal, electrodes. The arrows indicate the small deflexions (collateral potentials) associated with firing of the other lateral giant. In *c* and *d* simultaneous recordings were made from the two lateral giant segments of the same ganglion; a spike in one was accompanied by a small deflexion in the other. When a supraliminal current pulse was applied to the fibre on the right side (lower trace) the resulting spike failed to cross to the other side immediately, but gave rise to firing in that segment about 7·5 msec later. This delayed spike was presumably due to the impulse crossing to the left side in some distant ganglion. In *c* the late left-segment spike failed to cross back to the right side; but in *d* it did so and the cycle was then repeated twice.

spike a small deflexion (upper arrow) was recorded from the left fibre, followed 5·5 msec later by a conducted impulse; and this delayed spike was similarly accompanied by a small deflexion in the right segment (lower arrow). The small deflexions and the late firing on the left side can be attributed to the known cross-connexions between left and right lateral giants. In each ganglion the segmental neurone of one side sends a relatively small collateral branch

toward the mid line, where it makes synaptic connexion with a similar branch from the other side (Johnson, 1924; also see Methods). Thus the lateral giant system is a ladder-shaped network, with synapses not only between the segments of the 'uprights' (segmental synapses) but also in the centre of each 'rung'. These last junctions will be referred to as 'collateral' synapses to distinguish them from the segmental and giant motor synapses. The small deflexions shown in Fig. 5 would then, according to this explanation, be the 'collateral' post-synaptic potentials (p.s.p.'s) and the delayed firing of the left segment due to impulse transmission at a collateral synapse in some distant ganglion. The presence of collateral p.s.p.'s were an additional aid in identifying the lateral giant axons.

Another related property of the lateral fibre system which was sometimes observed, and which also helped in its identification, was a repetitive discharge following a single short stimulus. The records of Text-fig. 5*d* were taken from the same preparation and with the same electrode disposition as in *c*, but stimulation had been preceded by a longer period of rest. Rhythmic firing of this type can again be explained as a consequence of collateral synapses. Whereas the collateral p.s.p. in the right segment in *c* (lower arrow) failed to excite, it can be seen that in *d* a conducted spike appeared in the place of the p.s.p. and was presumably evoked by the latter. This second spike in the right segment was followed by a second action potential in the left segment, again after a delay due presumably to the impulse crossing at some distant ganglion. A number of sweeps had been superimposed in *d* and it can be seen that in some of them the cycle was repeated once more (the third spikes in each segment) but in others the second collateral p.s.p. did not succeed in reaching threshold. The third p.s.p. in the right segment failed to evoke a spike in all sweeps and repetition ceased. It should be pointed out that for an impulse to circulate in this way, around a loop of the lateral giant system, at least one of the collateral synapses must show effective one-way transmission. Otherwise, the impulse would cross at the first synapse and the two spikes would traverse the two segmental chains almost simultaneously, cancelling each other in the collateral branches. It can be seen that unidirectional transmission must have occurred in *d*, for the first spike on the right side was not followed by a contralateral impulse immediately, whereas the first left-segment spike did succeed in crossing with short delay. It seems highly probable that such one-way transmission in a system which appears to be anatomically symmetrical is due to injury and that the circuitous repetitive discharge is anomalous.

When two micro-electrodes were inserted into the same segment of a lateral giant axon, the relationship could be obtained between steady current applied through one electrode and membrane potential recorded with the other. Such current–voltage curves were required for the analysis of the GMS

described below. Examples are shown in Text-figs. 4 and 13*c*. Their shape and slope at the origin were characteristic of the lateral giant axons and contrasted with a typical curve obtained from a giant motor fibre (Text-fig. 13*d*). Provided that the distance between the two micro-electrodes was small in comparison to the length constant of the fibre, the slope at the origin of such a curve gives a measure of the input resistance, namely, the resistance between a point inside the fibre and the outside. The value of this slope for thirty lateral giant segments, each from a different preparation, was $1{\cdot}03 \pm 0{\cdot}05 \times 10^5\,\Omega$ (mean $\pm$ S.E.). The thirty experiments selected were those in which the distance between the current and voltage micro-electrodes was 0·2 mm or less, the mean distance being 0·14 mm. In eleven preparations a third electrode insertion was made and a rough measurement of the length constant (λ) obtained. The mean value ($\pm$ S.E.) was $1{\cdot}1 \pm 0{\cdot}1$ mm. It was useful to know this quantity in order to correct for errors due to the finite distance between current-passing and voltage-recording electrodes. For example, the above measurement of 'input resistance' should be increased by about 12% to compensate for the mean interelectrode distance of 0·14 mm.

The quantity λ is not strictly applicable to the lateral giant axon, which is segmented and part of a ladder-shaped network rather than a uniform cylinder of indefinite length. The error introduced by ignoring these features, however, is probably not large: (i) the measurements were usually made with the micro-electrodes more than a millimetre from the nearest segmental synapse (i.e. about one 'length constant' away); (ii), the electrical resistance of the segmental synapse appears to be low (unpublished observations); (iii) the nearest collateral branch was always beyond the segmental synapse (see Text-fig. 1) and its 'input resistance' probably high compared to the main part of the segment. Even if the lateral giant axon did not approximate to a linear cable, however, the apparent 'length constant' would still have been useful; for a similar disposition of the electrodes was used in obtaining 'λ' and in making the other measurements to which the correction for spatial decrement was applied.

The properties of the post-fibres. The post-fibre could be distinguished from any of the other fibres in the immediate neighbourhood by a number of physiological criteria. The first test was low-voltage stimulation of the third ganglionic root; and if the impaled axon fired, it was accepted as a third-root fibre. Text-fig. 6*a* shows such a direct response of an axon which was subsubsequently found to be the motor giant axon. In many experiments the impaled post-fibres were incapable of conducting nerve impulses and only graded local responses were obtained. But in either case it was assumed that a third-root fibre had been impaled and the next step was to test its response to stimulation of the nerve cord. If the axon was the motor giant axon, characteristic post-synaptic responses of the type shown in Text-fig. 6*b* were obtained. The two records, taken from different experiments, are multiple exposures and in b_1 the stimulating voltage was varied between sweeps. Provided that the shock intensity was sufficiently high, the early rapid deflexions were always followed by a slow potential (usually consisting of several summed components).

The early responses, as will be shown below, were evoked directly by the giant pre-fibres and were thus the p.s.p.'s of the giant motor synapses. They had an excitatory function and when supraliminal led to firing of the post-fibre. An example of such excitation is shown in *c*, in which cord stimulation intensity was varied while recording from the motor giant. The p.s.p. appeared in two steps, presumably associated with two different giant pre-fibres. In all but one of the sweeps, the summed p.s.p. evoked a post-fibre spike.

The size of the 'giant' p.s.p.'s varied, in different preparations, over a wide range from a few to over 40 mV. But in those cases in which they seemed to be larger than 25–30 mV there was probably a component of local response;

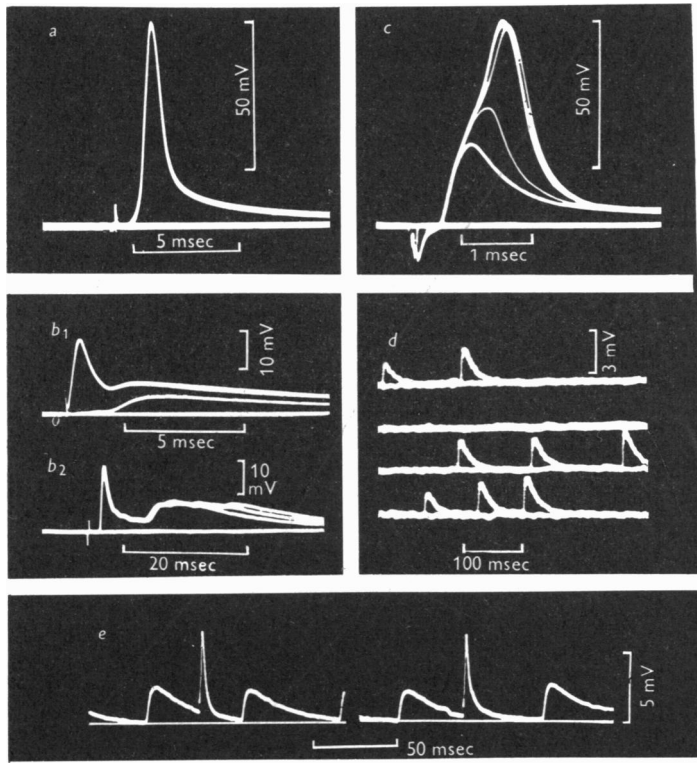

Text-fig. 6. Responses of the giant motor fibre. *a*, a directly evoked spike; the stimulus was applied to the third root by means of the capillary suction electrode. *b*, giant and slow p.s.p.'s following stimulation of the dorsal surface of the nerve cord. Multiple exposures. In b_1 the stimulus intensity was increased between successive sweeps. The pre-fibres for the slow response had the lowest threshold and only a slow potential is seen on the first sweep. *c*, a multiple exposure in which cord stimulation intensity was increased between sweeps. Two giant p.s.p.'s summed to evoke firing of the motor fibre. The record was retouched. *d*, slow potentials in the absence of stimulation. *e*, 'spontaneous' slow potentials and giant p.s.p.'s. The faster response in the centre of each trace was evoked by stimulation of the lateral giant pre-fibre. This 'giant' p.s.p. was among the slowest recorded. The base lines have been drawn.

for in many preparations the post-fibre was unable to conduct action potentials and only showed graded, local spikes. Nevertheless, at some synapses a single p.s.p. could cause firing of the post-fibre and thus effect one-to-one transmission. It seems likely that when the p.s.p.'s were small, this was the result of experimental damage (see Discussion).

TABLE 1. Post-synaptic potentials at the giant motor synapses

	Number of p.s.p.'s	Size (mV)	Rise time (msec)	Time from onset to half-decline (msec)
Lateral pre-fibres	28	17·9±1·4 (7–35)	0·45±0·02 (0·31–0·91)	1·4±0·1 (0·83–3·2)
Medial pre-fibres	8	13·4±1·6 (6–20)	0·41±0·03 (0·31–0·55)	1·2±0·1 (0·80–1·7)

The initial rate of rise of these p.s.p.'s was usually rather slow. In order to obtain a more consistent measure of the time of rise, the approximately linear portion of the rising phase was extrapolated to the base line and this point taken as the onset. Values have been determined separately for p.s.p.'s evoked by lateral and other (medial) giant pre-fibres. The range is given in brackets beneath the mean and S.E. The upper limit of the range of rise times (0·91 msec) for lateral giant p.s.p.'s was considerably larger than the next-to-highest value, which was 0·58 msec.

The time course of the 'giant' p.s.p.'s is summarized in Table 1. P.s.p.'s which were not associated with firing of the lateral giant axon were assumed to be due to either of the medial pre-fibres (see Methods). Although p.s.p.'s can also be evoked by the contralateral segmental axon, such responses can be recognized by their small size and long latency (see below) and they have not been included in the table. The time courses of the two groups of p.s.p.'s (Table 1) were not significantly different. In both cases the rising phase was usually complete in less than 0·5 msec and the decline from peak to half-peak occurred, in most cases, within 1 msec. By contrast, the p.s.p.'s recorded from some of the smaller fibres of the third root were considerably slower. The mean rise-time for twelve such responses was 1·5 msec (1·0–2·5) and the time from onset to half-decline was 7·3 msec (3·5–15·6).

The other characteristic response of the motor giant, the late slow potentials shown in Text-fig. 6*b*, is considered in detail in the following paper (Furshpan & Potter, 1959). Evidence is presented that these potentials are associated with inhibitory effects, despite the fact that they almost always appeared as depolarizations. The difference in their physiological effect, as well as that in time course and latency, makes the slow potentials easily distinguishable from the 'giant' p.s.p.'s.

In addition to these two types of response following cord stimulation, intermittent slow deflexions were seen in most giant post-fibres in the absence of any applied stimulus (Text-fig. 6*d*). Observations discussed in the following paper (Furshpan & Potter, 1959) indicate that the spontaneous potentials are due to firing of the same pre-fibres which evoke the late, slow responses. In Text-fig. $6b_2$ the variability in the slow potential is attributable to enhanced firing of the 'spontaneous' potentials following cord stimulation. Text-fig. 6*e* allows a comparison between the time courses of a 'giant' p.s.p. and the spontaneous potentials. Cord stimulation was adjusted so that the only pre-fibre to fire was the ipsilateral segmental giant fibre and the resulting post-

fibre response appears in about the centre of each trace. The smaller, slow deflexions are the spontaneous p.s.p.'s. The contrast between the time courses of the two potentials was less than that usually observed. The main point to be emphasized about the above observations, however, is that the spontaneous potentials and the typical pattern of fast and slow responses to cord stimulation were singularly characteristic of the giant motor fibre and allowed it to be distinguished from any of the other axons that were impaled in these experiments.

Following the insertion of a second micro-electrode into the motor giant axon, the current–voltage relationship, as described above, could be obtained. A typical curve (Text-fig. 13*d*) differed from that for the pre-fibre in several respects. (1) The post-fibre curve appeared to deviate more markedly from linearity for similar changes of membrane potential. (2) With inward membrane current (the lower left quadrant) the curvature was opposite for the two fibres. (3) The slope at the origin was steeper for the post-fibre, the mean value in eleven experiments being $6{\cdot}0 \times 10^5\ \Omega$. A large fraction of the higher 'input resistance' is accounted for by the smaller size of the post-fibre and at least part of the opposite curvature found for inward currents (see (2) above) is due to the presence of the GMS, as will be explained below. If these factors are taken into account the discrepancies between the curves for pre- and post-fibres are considerably reduced. Their observed shapes are, however, characteristic and additional means of distinguishing the fibres. Because of the difficulty of impaling the motor giants, a measurement of characteristic length, which requires at least three insertions, was infrequently made and then probably involved considerable error due to damage of the fibre.

Orthodromic nerve-impulse transmission

When micro-electrodes were inserted into both pre- and post-fibres, the succession of potential changes in the two axons could be recorded during an action potential in either. Examples of transmission from pre- to post-fibres (orthodromic) are shown in Text-fig. 7, in which pre-fibre membrane potential always appears on the upper trace of each pair. In a few experiments one-to-one transmission occurred (Text-fig. 7*a*), but in most only a p.s.p. was seen in the post-fibre (*b*). In *a*, the inflected rising phase of the post-fibre spike is similar to that seen in action potentials recorded from other post-junctional regions (e.g. the motor end-plate (Fatt & Katz, 1951)).

The most striking aspect of these records is the brevity of the delay between the foot of the pre-fibre spike and the start of the p.s.p. The initially low rate of rise of both pre- and post-fibre potentials makes the assessment of this delay difficult; in some cases the two potentials seemed to arise at about the same time but at different rates. In order to obtain a measure of delay, the approximately linear parts of the rising phases pre-fibre spike and p.s.p. were extrapolated to the base line. The time between the two points of intersection, in thirty-one experiments (all on lateral GMS's), was $0{\cdot}10 \pm 0{\cdot}01$ msec

(mean ± S.E.). Taking pre-fibre spike conduction velocity as 5 m/sec (mean of four experiments) a correction was made for the conduction time between pre-fibre micro-electrode and synapse. The corrected delay was 0·12 ± 0·01 msec (range, 0·07–0·02 msec).

In both *a* and *b* the lateral giant axon had been stimulated by means of an external capillary electrode applied to the surface of the cord. The measure-

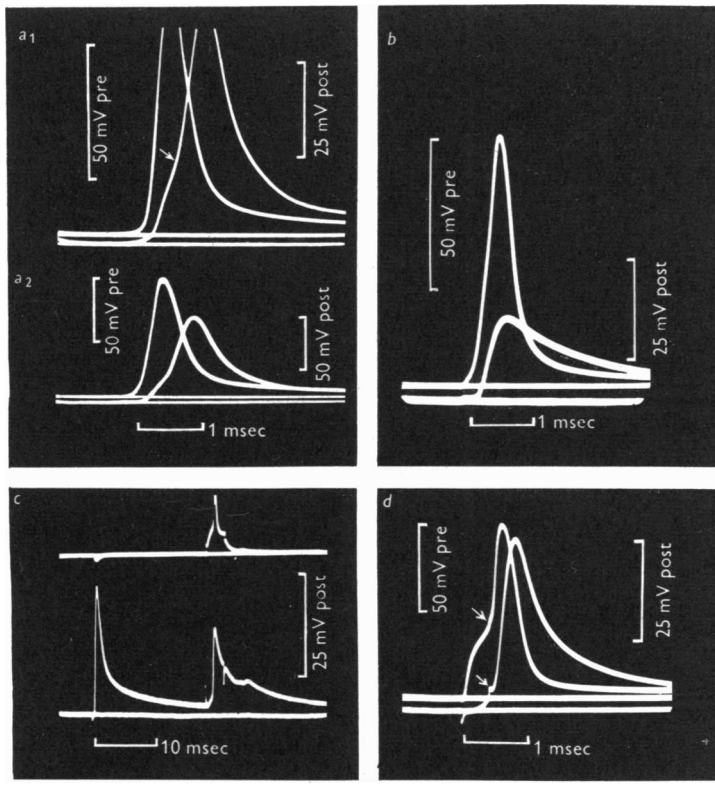

Text-fig. 7. Orthodromic nerve-impulse transmission at the GMS. Simultaneous intracellular recordings from pre- and post-fibres. In each case pre-fibre potential was recorded on the upper trace. The second p.s.p. in *c* and that in *d* were evoked by direct stimulation of the pre-fibre with an intracellular electrode; otherwise the stimulus was applied externally to the dorsal surface of the cord. a_1 and a_2 were recorded from the same synapse at different amplifications. The p.s.p., at about the point indicated by the arrow in a_1, exceeded threshold and evoked a spike. The upper part of the rising phase of the prespike was retouched. Sub-threshold p.s.p.'s are shown in *b–d*. In *c*, the first p.s.p., evoked by external stimulation, was apparently due to firing of one of the medial giant fibres, for no spike was seen in the impaled lateral giant fibre (upper trace). The second p.s.p. accompanied a lateral giant spike (85 mV) evoked by intracellular stimulation. The small hump on its falling phase was probably associated with firing of the other lateral giant fibre. *b* and *c* were recorded from the same synapse, but the polarity of the external stimulating pulse was opposite in the two cases. In *d* the arrows indicate the end of the depolarizing current pulse applied to the pre-fibre.

ment of synaptic delay would be invalid if a giant pre-fibre, other than the impaled one, were to fire first and give rise to an earlier p.s.p. To eliminate this possibility, the stimulus strength was varied in order to confirm that both pre- and post-fibre responses had identical thresholds. This was indeed the case in Text-fig. 7*a* and *b*. Nevertheless, the possibility remained that the thresholds of two of the giant pre-fibres were too close to be distinguished. A more decisive procedure was to stimulate the pre-fibre selectively with a second internal electrode. Fig. 7*c* illustrates a situation in which the internal stimulating electrode was particularly useful. A stimulus to the cord just strong enough to evoke a giant p.s.p. (first response on the lower trace) failed to excite the impaled lateral giant axon (upper trace). This post-fibre response was presumably evoked by one of the medial giant axons. Later during the same sweep the lateral giant axon was stimulated by means of an intracellular electrode, and the resulting action potential was accompanied by another p.s.p. In this case one can feel confident that the second p.s.p. was due to the firing of the impaled lateral giant axon and that the short synaptic delay was real. The record of Text-fig. 7*d*, taken at higher sweep speed, shows another example of transmission following intracellular stimulation of the pre-fibre. Although the presence of the pulse complicates the estimation of the synaptic delay, it is clear that the delay was very small.

An incidental observation is also illustrated in Text-fig. 7*c*. The small, late deflexion seen on the falling phase of the second p.s.p. was approximately coincident with a collateral p.s.p. in the lateral giant axon. This has also been observed in three other experiments and suggests that the late deflexion is associated with the contralateral segment of the lateral giant axon. In one of these experiments simultaneous recordings were made from a motor giant axon and the contralateral segmental giant axon. When the ipsilateral segmental giant axon was stimulated by means of an internal electrode, an action potential subsequently appeared in the contralateral segment (as in the case illustrated in Text-fig. 5). It was then seen that this contralateral action potential was approximately coincident with the late deflexion in the motor fibre. Such a coincidence, however, is only suggestive of a causal relationship. If such a relationship exists there are two synapses, reported in histological studies, which might account for the late deflexion. The first (Johnson, 1924) is between the motor giant axon and the collateral branch of the contralateral segmental giant axon, while the second (Robertson, 1955) is between the two opposite motor giant axons. In the second case, for example, the complete pathway would be from ipsilateral to contralateral segmental giant axon, from there to the contralateral motor giant axon and only then to the ipsilateral motor giant axon.

Tests for the presence of antidromic transmission

Wiersma (1947) found that in *Cambarus* stimulation of the third ganglionic root did not evoke firing of any of the giant pre-fibres. A similar test for antidromic transmission has been made in the present experiments but using intracellular recording. Text-fig. 8*a* illustrates the type of result obtained in the six experiments in which internal electrodes had been inserted on either side of a GMS, and in which the post-fibre showed an all-or-nothing action potential. The motor fibre was stimulated directly by means of the capillary electrode

containing the third root. In the case shown in Text-fig. 8*a* the magnitude of the post-fibre action potential was 77 mV, while the size of the small accompanying deflexion in the lateral pre-fibre was less than 0·3 mV. The post-fibre spike was thus 250–300 times as large as the consequent pre-fibre potential change. It will be convenient to refer to this ratio as the attenuation factor. Text-fig. 8*b* shows a record of orthodromic transmission at the same synapse.

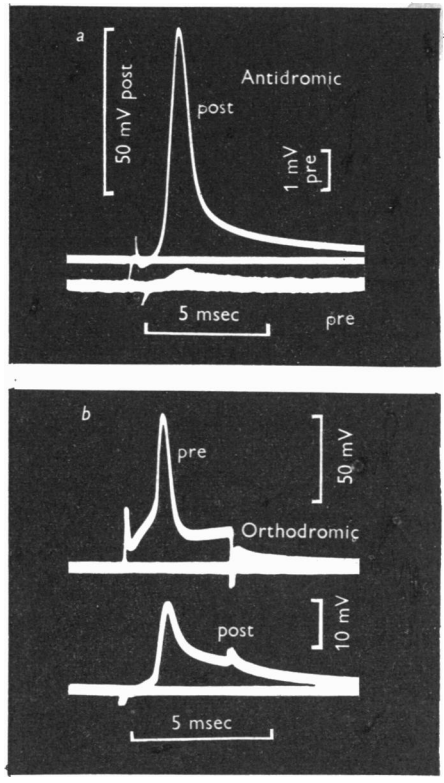

Text-fig. 8. A comparison of the effects of orthodromic and antidromic nerve impulses at the same synapse. Simultaneous intracellular recording from both synaptic elements following stimulation of the post-fibre in *a* and the lateral giant pre-fibre in *b*. The pre-fibre stimulus was applied through a third intracellular electrode.

The lateral giant axon was selectively stimulated by means of a second internal electrode and a pre-fibre spike of 83 mV gave rise to a p.s.p. of 18·5 mV. In this case the attenuation factor was about 4·5. The transmission mechanism was, therefore, about 60 times as effective in the orthodromic as in the antidromic direction. In two other experiments of this type the ratio of antidromic to orthodromic attenuation factors was 210:3·9 = 54 and 350:2·8 = 125. In another two cases the pre-fibre deflexions were too small to be measured at the amplifications used, but were less than 0·3 mV. Thus in five of these six

experiments the synapse was highly 'directional', the ratio of attenuation factors being greater than fifty. In the remaining case an appreciable antidromic effect was seen and the attenuation factor ratio was about three; but this synapse was atypical in another important respect, the consideration of which will be deferred to the Discussion. That there is usually no significant antidromic transfer has also been confirmed in twelve additional experiments in which an intracellular electrode was placed only in the pre-fibre. In every case relatively large stimuli applied to the third root resulted in pre-fibre deflexions of less than 1 mV; but in the absence of intracellular recording from the post-fibre there could be no assurance that a conducted, antidromic spike had been evoked.

Tests for the transfer of electrotonic potentials across the synapses

It has been seen that an action potential in the pre-fibre could give rise to a p.s.p. of 25 mV or more. The question then arose whether smaller, or even subthreshold, depolarizations of the pre-fibre would also bring about an appreciable transynaptic effect (i.e. in the post-fibre); and whether local electrotonic alterations in the membrane potential of the post-fibre would have as little effect on the pre-fibre as did the antidromic nerve impulse. In order to test these questions, experiments were made initially with one internal electrode in each synaptic element. Either micro-electrode could be used to pass pulses of current while the other recorded any changes in the membrane potential of the transynaptic fibre. It was found that even subthreshold current pulses applied to the pre-fibre could, in fact, give rise to considerable potential changes in the giant motor fibre and the transynaptic effect had the appearance of an electrotonic potential (Text-fig. 9*a*). A marked effect was only present, however, when the direction of the current across the pre-fibre membrane was outward (i.e. causing depolarization). Any post-synaptic effects produced by inward (hyperpolarizing) currents were very much smaller (Text-fig. 9*b*).

The experimental situation was then reversed, the post-fibre electrode being used to pass current while the pre-fibre electrode recorded potential changes. Now it was found that depolarizing currents applied to the motor giant axon had very little effect on the pre-fibre potential (Text-fig. 9*c*); but, most unexpectedly, hyperpolarizing currents were seen to produce marked transynaptic effects, which had the appearance of anelectrotonic potentials (Text-fig. 9*d*). To summarize, transynaptic membrane potential changes were observed only if depolarizing current was applied directly to the pre-fibre or hyperpolarizing current to the post-fibre. In order to have convenient terms with which to distinguish the experimental situations considered above, the words 'orthodromic' and 'antidromic' will be used, in analogy with nerve-impulse transmission. The orthodromic situation is that in which current is passed with the pre-fibre electrode and the electrotonic potentials appear to

cross the junction from pre- to post-fibre. In the antidromic case the current-passing electrode is, of course, in the post-fibre. One can now restate the above observations as follows. Only depolarizations cross the synapse orthodromically in appreciable amounts while only hyperpolarizations do so antidromically.

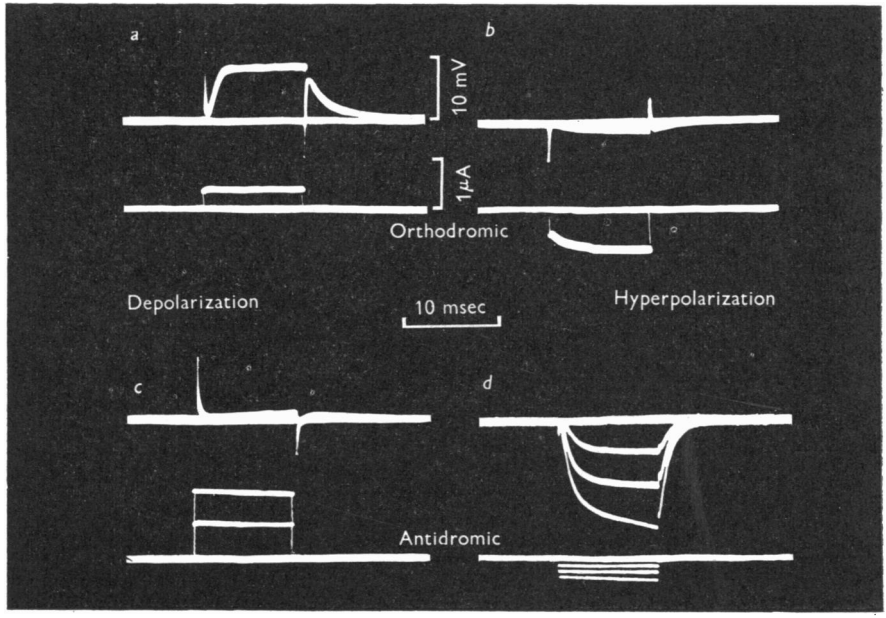

Text-fig. 9. Tests for transynaptic effects of applied current pulses. Inward and outward currents were successively applied to each fibre while recording the membrane potential of the other. The current was applied to the pre-fibre (orthodromic situation) in *a* and *b*, and to the post-fibre in *c* and *d*. The current pulses are shown on the lower, membrane potential on the upper trace of each pair. Outward current and depolarization appear as upward deflexions. The depolarizing pulse in *a* was just below pre-fibre threshold. The calibrations apply to all four cases. The records have been retouched.

Confirmation of these results has been obtained in thirty out of thirty-two experiments in which at least one micro-electrode had been inserted on either side of the junction, and in which both orthodromic and antidromic pulse transmission was tested. In the two experiments which did not conform to this pattern, potential changes of the appropriate sign were seen in one synaptic fibre when current of either direction was applied to the other. One of these two was the experiment mentioned above, in which the ratio of antidromic to orthodromic attenuation factors was very low, about 3.

The synaptic–rectifier hypothesis

The seemingly diverse results of Text-fig. 9 can all be explained by a single mechanism embodied in the following hypothesis: The junction operates by

means of 'electrical' transmission, the transynaptic effects seen in Text-fig. 9*a* and *d* resulting from a portion of the applied current crossing the junction; and it behaves like an electrical rectifier, accounting for the negligible transfer of the pulses in *b* and *c*. The hypothesis is illustrated in Text-fig. 10, which shows the direction of flow of current associated with the four experimental situations of Text-fig. 9. Some of the current applied to one fibre must also cross the membrane of the other, by way of the synapse, the amount varying with the 'synaptic resistance'. It is apparent that in the two situations (*a*, *d*),

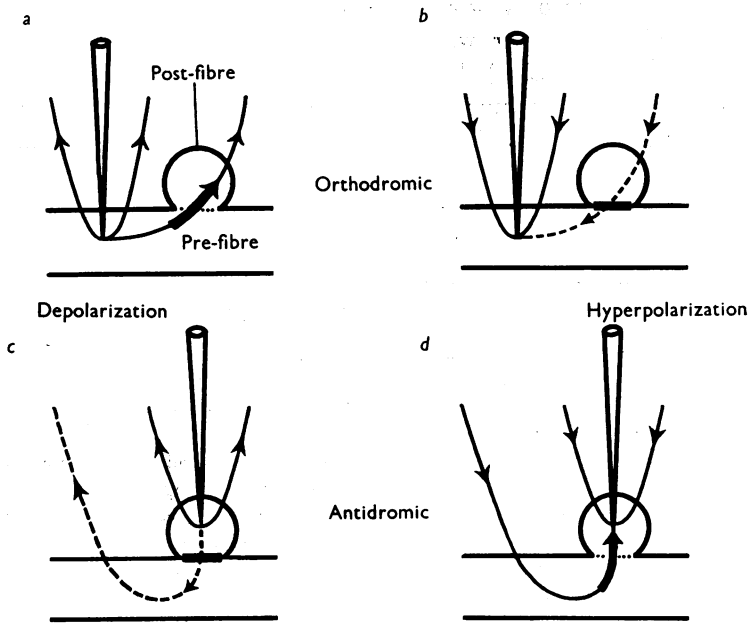

Text-fig. 10. The synaptic-rectifier hypothesis. The diagrams correspond, in the same order, to the four experimental situations of Text-fig. 9. The post-fibre is shown in transverse section at the point at which it crosses over the pre-fibre; the junction is indicated by a dotted line or a heavy bar, representing a low or high synaptic resistance, respectively. The arrows give the direction of (positive) current entering or leaving the current-passing micro-electrode; dashed lines indicate negligible current flow due to high synaptic resistance. Diagrams *a* and *d*, corresponding to the two situations in which transynaptic effects were observed, show that in both cases current would cross the junction in the same direction (indicated by the heavy arrows.)

in which there were considerable transynaptic effects, the direction of any synaptic current was the same, and opposite to that in the other two cases. Therefore, if the synapse were an electrical rectifier and only allowed appreciable (positive) current to cross it in the direction shown by the heavy arrows (Text-fig. 10*a*, *d*) the above results would be explained. The dashed lines (*b*, *c*) indicate that the amount of current flow would be negligible, thus accounting for the absence of transynaptic potential changes in those cases.

An alternative statement of the hypothesis is given in the circuit diagram of Text-fig. 11. For simplicity the two synaptic elements are shown as if they were in line and terminated at the point of juncture, rather than crossing each other (as shown in Text-fig. 1). R_{pre} and R_{post} represent the 'input resistances' of the two fibres. The insides of the axons are separated by the synaptic resistance, S, which is shown as a rectifier. It is apparent that any change in potential across R_{pre} would also alter the p.d. across R_{post}, and vice versa, provided that S is not extremely large. To explain the results of the above experiments, S is assumed to be low only when the inside of the pre-fibre becomes more positive (depolarization) or when the post-fibre becomes more internally negative (hyperpolarization). That is, both situations give rise to a p.d., across the synapse, of the same sign; and the rectifier is assumed to have a low resistance for p.d.'s of this direction (indicated by the plus and minus signs Text-fig. 11.).

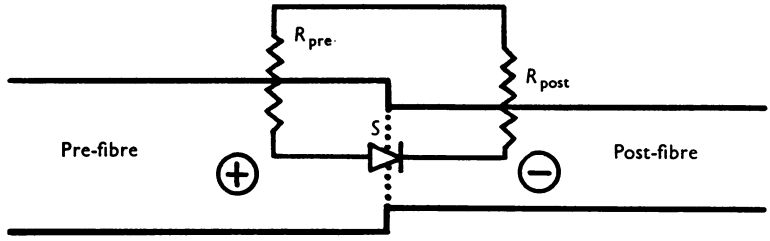

Text-fig. 11. The proposed equivalent circuit for the GMS. Pre- and post-fibres are shown as though terminating end to end (see Text-fig. 1, however). The 'input resistances' of the two fibres are represented by the elements, R_{pre} and R_{post}; and the synaptic resistance by S. The plus and minus signs indicate the direction of the p.d. across the junction for which S is small. Inasmuch as R_{pre} and R_{post} are shown as constant resistive elements, the diagram only holds for small steady potential changes.

Tests of the synaptic–rectifier hypothesis

The current–voltage relationship of the synapse. If the junction behaves like a simple rectifier in an electrical circuit, and the observed transynaptic effects are due entirely to passive current flow across it, the intensity of this synaptic current should depend only on the p.d. across the rectifier, but not on the way in which the p.d. is brought about. In other words, the current–voltage characteristic of the junctional rectifier should account equally well for the transynaptic effects seen in the orthodromic and antidromic situations. In the absence of a direct measure of the current traversing the synapse, however, the rectifier characteristic cannot be directly determined. Instead, we have separately calculated two experimental current–voltage curves for the synapse, one for the orthodromic situation and one for the antidromic. Each characteristic was constructed so that it would exactly account for the transynaptic effects seen in that situation. Comparison of the two curves then provided

a critical test of the hypothesis; for if they were the same, it would mean that a synaptic rectifier with that current–voltage characteristic would quantitatively account for the diverse results of the current-passing experiments.

The following data were used in making the required calculations: recordings of membrane potential from both fibres during the application of various currents to each, in turn; and the current–voltage relationships of the two fibres. The most satisfactory method for obtaining this information was to insert a pair of micro-electrodes, for passing current and recording potential, into each synaptic element, thus avoiding the necessity of withdrawing or inserting electrodes during the course of the measurements. Text-fig. 12 shows part of the required data from one experiment, namely simultaneous records of membrane potential from the two fibres of a GMS. The potential changes in *b* and *d* are the transynaptic effects accompanying the directly evoked electrotonic potentials on the other side of the junction (*a* and *c*). The results confirm those obtained in the two-micro-electrode experiments (e.g. Text-fig. 9); but they also allow the p.d. across the synapse to be found, as well as providing a measure of the voltage attenuation across the junction (see below). The current–voltage curves for the synaptic elements, from the same experiment, are shown in Text-fig. 13*c* and *d*. The graphs in *a* and *b* are essentially the same results as those in Text-fig. 12, but displayed in a more convenient way. In *a* current was applied to the pre-fibre while recording the membrane potentials of pre- and post-fibres on the abscissa and ordinate, respectively; *b* shows the analogous results for the antidromic situation. The four curves of Text-fig. 13 provide the necessary data for making the two separate determinations of the apparent current–voltage characteristic of the synaptic rectifier.

The following symbols have been used. V_s and I_s represent changes from the resting values respectively of the p.d. across the junction and of the apparent current traversing it. V_{pre} and V_{post} denote changes in the internal potentials, with respect to the bath, of the two synaptic elements. (Changes in potential and current were used because the resting values were not always known.) The voltage across the synapse is equal to the difference between the local internal potentials of pre- and post-fibres in the immediate vicinity of the junction; and the sign of V_s is taken so that $V_s = V_{pre} - V_{post}$. Since V_{pre} and V_{post} are positive for depolarizations of the fibres, V_s is positive when directed as in Text-fig. 11.

The method of analysis is illustrated in Text-fig. 14. In this example V_s and I_s will be determined for an orthodromic case in which the pre-fibre was depolarized by 30 mV. *a* and *b* are tracings of Text-fig. 13*a* and *d*. It can be seen in *a* that for $V_{pre} = 30$ mV, $V_{post} = 10{\cdot}6$ mV; and $V_s = V_{pre} - V_{post} = 19{\cdot}4$ mV. In determining I_s it was assumed that the transynaptic potential change (in this case V_{post}) was the result of the synaptic current I_s flowing across

the 'input resistance' of the post-fibre (R_{post}; see Text-fig. 11). Thus, $I_s = V_{post}/R_{post} = I_{post}$; and the relevant value of I_{post} can be found from the current–voltage curve for the post-fibre. This has been done in Text-fig. 14*b*, giving a value for I_s of $2{\cdot}2 \times 10^{-8}$ A. Perhaps a simpler way of describing the determination of I_s is the following: the amount of current which must be injected into the post-fibre at a point, in order to reproduce the transynaptic potential change (10·6 mV), was found from the current–voltage curve of the fibre to be $2{\cdot}2 \times 10^{-8}$ A. The assumption was made that the two situations, namely, of current entering the post-fibre through the synapse or through a current-passing micro-electrode, are equivalent; and that all of the current crossing the junction entered the post-fibre. The determination of V_s and I_s was then repeated for pre-fibre depolarizations of different sizes. The filled-in

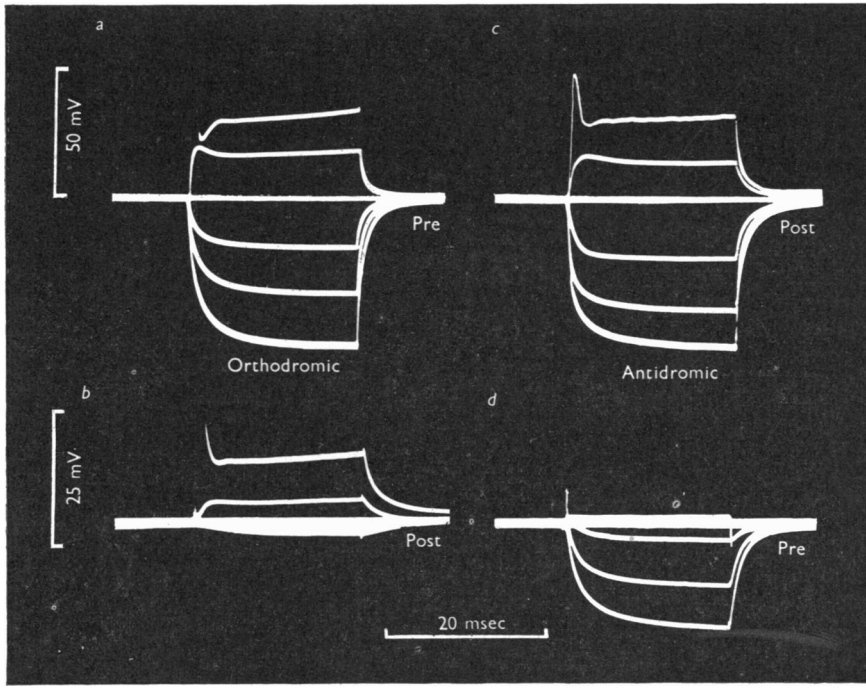

Text-fig. 12. Tests for the transmission of electrotonic potentials across the GMS. The membrane potentials of pre- and post-fibres were simultaneously recorded while applying steady pulses of current, by means of another internal electrode in each axon, to the pre-fibre (*a* and *b*) or post-fibre (*c* and *d*). The direct electrotonic potentials, *a* and *c*, are shown above the corresponding transynaptic effects, *b* and *d*. Deflexions above the base line are depolarizations. The larger catelectrotonic potential in *a* was above threshold, but most of the resulting spike and the accompanying p.s.p. (in *b*) are not visible in the records. The response in *c* was a graded, local spike. Voltage calibrations in *a* and *b* also apply, respectively, to *c* and *d*; the time calibration applies to all records.

circles in Text-fig. 15 give the values obtained for changes in V_{pre} in steps of 5 mV, over the range 0–50 mV. The various points were determined using the upper right quadrants of the curves in *a* and *d* of Text-fig. 13 and the point indicated by the arrow is the one derived in the above example. The open circles in Fig. 15 were obtained from the same experiment for hyperpolarizations in the antidromic situation. V_s and I_s were determined in a way analagous to that just described, but using the lower left quadrants of graphs *b* and

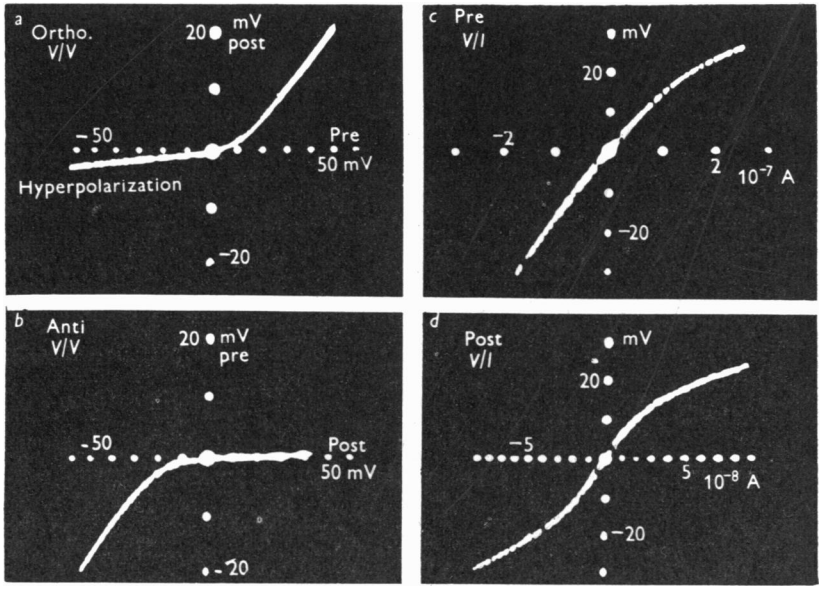

Text-fig. 13. The data necessary for determining the current–voltage characteristic of the synapse in two independent ways. *a* and *b* provide the same type of information as Text-fig. 12, but more completely and in a more convenient form. The membrane potentials of the two fibres were recorded, one on each co-ordinate axis of the oscilloscope, while varying the current applied to the pre-fibre (*a*) or post-fibre (*b*). The potential of the fibre to which the current was directly applied is on the abscissa. *c* and *d* are the nominal (see Discussion) current–voltage curves of pre- and post-fibre. The current was applied with an internal electrode and membrane potential measured nearby, also intracellularly. In all records the method of varying the applied current was that used in Text-fig. 4*a*. Depolarizations and outward membrane currents appear in the upper right quadrant. From the same experiment as Text-fig. 12.

c of Text-fig. 13. The points are those found for alterations in V_{post}, in steps of −5 mV, from 0 to −50 mV. The almost complete agreement between the two relations leaves little doubt of the correctness of the synaptic–rectifier hypothesis, and confirms that the currents that were assumed to cross the synapse, in order to account for the transynaptic effects, were in fact doing so. On any other hypothesis it would be very difficult to understand why the

apparent synaptic currents should be identical, during pre-fibre depolarizations and post-fibre hyperpolarizations, whenever the two happened to bring about the same potential difference across the synapse. This is, of course, just the result to be expected if the junction behaved like an electrical circuit element of the kind represented in Text-fig. 11.

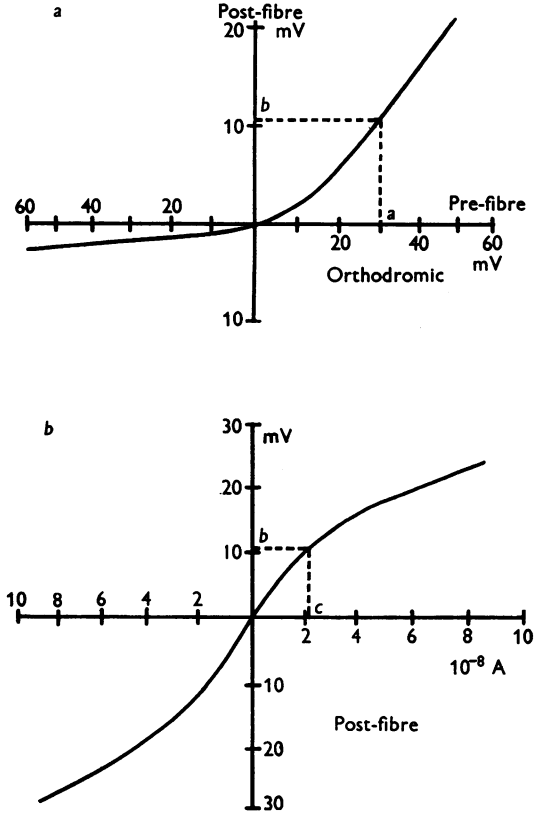

Text-fig. 14. The determination of V_s and I_s. *a* and *b* were traced, respectively, from Fig. 13*a* and *d*. $V_s = V_{pre} - V_{post}$; for $V_{pre} = 30$ mV, $V_{post} = 10{\cdot}6$ mV and thus $V_s = 19{\cdot}4$ mV. I_s was found by a substitution method: that current which duplicated the transynaptic effect, when applied directly to the post-fibre through a micro-electrode, was taken as equal to I_s. The value found from *b* was $2{\cdot}2 \times 10^{-8}$ A.

Curves relating V_{pre} to V_{post} (Text-fig. 13*a*, *b*) do not, by themselves, give an accurate measure of synaptic rectification; for their shape also depends on the membrane properties of the transynaptic fibre. But in deriving the I_s/V_s curve the non-linearities of the individual fibre membranes were eliminated, and Text-fig. 15 represents rather accurately the rectifier properties of the synapse itself. The figure shows only the characteristic for positive values of V_s, so that the resistance of the junction in the forward and reverse directions

cannot be compared; but some measure of the degree of 'rectification' is that the 'slope conductance' (dI_s/dV_s) at $V_s = 30$ mV is approximately fifty times that at the origin.

Points relating V_s to I_s were also determined in the same experiment, for the two situations in which V_s was negative (i.e. 'orthodromic hyperpolarizations' and 'antidromic depolarizations'). General agreement between the two sets of points was found for these cases as well. The values of $-I_s$ against $-V_s$, together with the open circles in Text-fig. 15, were used to draw the more complete characteristic curve for the synapse shown in Text-fig. 16.

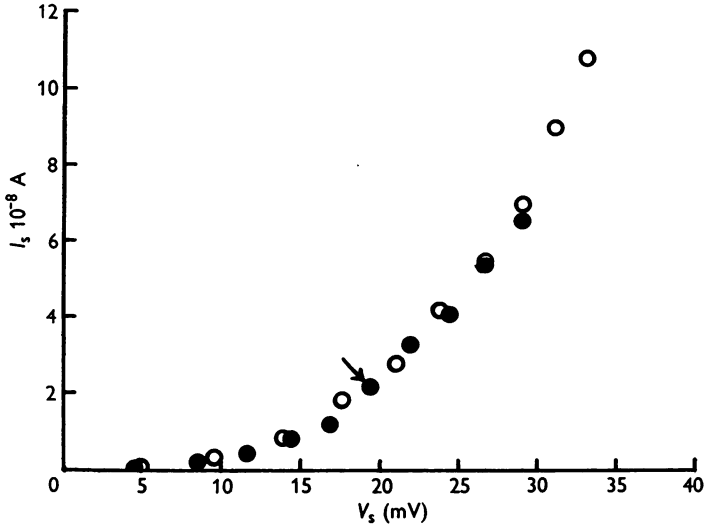

Text-fig. 15. The current–voltage characteristic of the synaptic rectifier for the forward direction only. ●, points determined for orthodromic depolarizations using the curves of Text-fig. 13*a* and *d*. The arrow indicates the point calculated in Text-fig. 14. ○, points obtained for antidromic hyperpolarizations from Text-fig. 13*b* and *c*. Both sets of points were found for increments of 5 mV, up to a change of 50 mV, in the membrane potential of the fibre to which the current was directly applied.

The ratio of the 'slope conductance' at $V_s = -30$ mV to that at the origin is one-third to one-quarter, so that the ratio of slopes compared at $V_s = 30$ and -30 mV was 150 or more. The ratio of 'chord conductances', I_s/V_s, at the same two values of V_s was about 35. Too much emphasis must not, however, be placed on the negative part of the curve in Text-fig. 16. There was considerable uncertainty in estimating such small synaptic currents, although the true values of I were probably not larger than those shown in the figure.

Of the thirty-two experiments mentioned above, fourteen were made with two micro-electrodes in each fibre and these provided sufficient information to construct the two synaptic–rectifier curves. General agreement between I_s against V_s for 'orthodromic depolarizations' and 'antidromic hyperpolarizations' was found in all fourteen cases, but in most of them the correspondence

was not as precise as that illustrated in Text-fig. 15. Probably the most important variable influencing such agreement was the spatial decrement of electrotonic potentials from their site of origin (the synapse or one of the current-passing micro-electrodes) to the point at which they were measured. Usually these distances were 10–20% of the 'characteristic lengths' of the fibres. Depending on the positions of the micro-electrodes, however, the discrepancy between the orthodromic and antidromic situations could either be reduced, owing to equal errors in the two cases, or magnified by one or both of

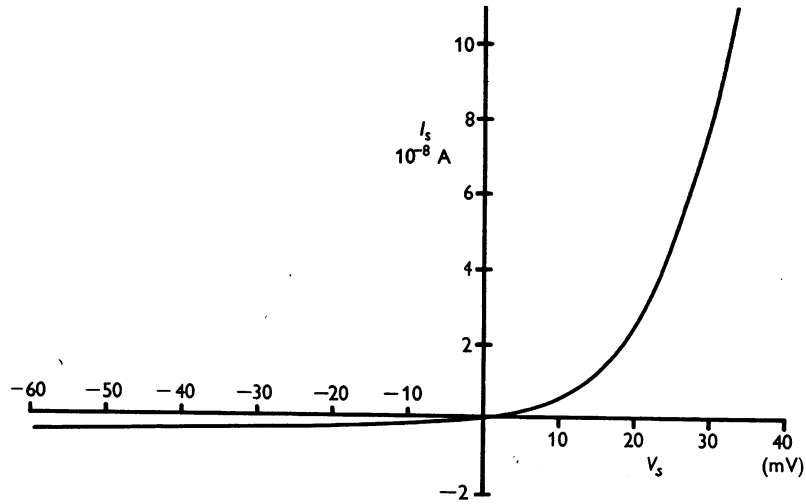

Text-fig. 16. The complete current–voltage characteristic of the synaptic rectifier. Positive values of V_s signify that the pre-fibre side of the junction was electrically positive with respect to the post-fibre side. Taken from the same experiment as Text-figs. 12–15.

the following factors. (1) The membrane resistance, and thus also the spatial attenuation, alters with the level of membrane potential of the fibres; an appreciable decrease in membrane resistance and an increase in spatial attenuation occur with either large depolarizations of the pre-fibre or large hyperpolarizations of the post-fibre (see Text-fig. 13*d*). (2) Since $V_s = V_{pre} - V_{post}$, an error in V_{pre} in the orthodromic case, for example, will give rise to a still larger percentage error in V_s. This point may be illustrated using the experiment of Text-fig. 14. A depolarization of the pre-fibre of 50 mV gave rise to a change in post-fibre potential of 21 mV. The apparent value of V_s was therefore 29 mV. Suppose that the measured value of V_{pre} had been 15% too large, owing to decrement of the catelectrotonus between voltage-recording electrode and synapse; then the true value of V_s would have been 22·5 mV (43·5–21 mV) rather than 29 mV, and the above estimation of V_s would have been 29% too large. This exaggeration of the error in calculating V_s is less for

smaller depolarizations, for then the transynaptic potentials are relatively smaller. This type of error was probably less important for the antidromic case, for the post-fibre electrodes were usually closer to the synaptic region. The errors in the current–voltage curves of each fibre, caused by spatial attenuation, were less serious. There was no amplification of the inaccuracy and the percentage error tended to be about the same for both fibres, so that both the orthodromic and antidromic situations were affected to about the same extent and in the same direction.

In six out of the total of fourteen four-electrode experiments, the agreement between the synaptic current–voltage curves for orthodromic depolarizations and antidromic hyperpolarizations was very good without making any corrections for electrotonic decrement along the fibres. Any discrepancy between the two curves in these experiments could be corrected by a change in V_s of 10% or less. In view of the sensitivity of these curves to small inaccuracies in V_{pre} and V_{post}, some of this impressive agreement was probably due to fortuitous balancing of errors in the orthodromic measurements by those in the antidromic. In another six experiments the disparity between the two curves was greater, but was in the direction to be expected if it were due to the spatial decrement of the electrotonic potentials. In none of these cases was there sufficiently complete information on the 'characteristic lengths' of the fibres to make exact corrections. In all, however, it was possible to eliminate the discrepancies between the curves by correcting V_{pre} using reasonable assumed values for 'λ', or by basing corrections for V_{post} on the difference between the sizes of the p.s.p.'s recorded at the two electrodes. The magnitudes of pre-fibre 'λ' which had to be assumed all fell within the range of values found in other experiments.

Of the remaining two experiments, one could not be satisfactorily corrected by the above procedure and the other was one of those in which the synapse showed almost no rectification. In the first of these two experiments, even after assuming a pre-fibre 'λ' as low as 0·5 mm and correcting V_{post} for the difference in the p.s.p.'s recorded at the two electrodes, there remained a disparity of about 20% between the two values of V_s at a given I_s. The difference between the p.s.p.'s recorded at the two post-fibre electrodes was rather large, one being 40% greater than the other for an electrode separation of 0·14 mm; and it seems likely that one of these electrodes was not properly inserted. Despite this disparity, the general shapes of the orthodromic and antidromic curves were quite similar.

In the remaining experiment the almost complete absence of synaptic rectification introduced an error which precluded an accurate analysis of I_s against V_s without additional information. The point is worth considering, for it illustrates how the presence of the synaptic rectifier in the other experiments simplified the investigation. The apparent current–voltage relationship of each fibre was determined with the micro-electrodes in the junctional region, so that the applied

current took two parallel pathways. In the case of the post-fibre, for example, some of the applied current, I, flowed across the synapse as well as across the post-fibre membrane (i.e. $I = I_s + I_{post}$). Graphs of the type shown in Text-fig. 13*d* relate V_{post} to I; but for the above analysis the relationship between V_{post} and I_{post} was required. The size of this error ($I - I_{post}$) depends on the extent of shunting by the synapse (i.e. on I_s). Since I_s was very small during pre-fibre hyperpolarizations and post-fibre depolarizations, these parts of the current–voltage curves were not much affected by the proximity of the junction. For example, in the experiment of Text-fig. 13*d*, $6{\cdot}2 \times 10^{-8}$ A of outward current applied to the post-fibre gave a depolarization of 20 mV. The fraction of this current which left the post-fibre by way of the synapse can be estimated as above. Referring to Text-fig. 13*b*, when V_{post} was 20 mV, V_{pre} was less than 0·3 mV. From the pre-fibre current–voltage curve, Text-fig. 13*c* (slope at the origin $= 1{\cdot}5 \times 10^5\ \Omega$), it was found that an applied current of about $0{\cdot}2 \times 10^{-8}$ A was needed to reproduce $V_{pre} = 0{\cdot}3$ mV. This does not give an exact measurement of I_s, however, since the pre-fibre curve is also in error owing to shunting by the synapse; but the direction of the error is such that the true value of I_s would be smaller than that found. Thus, $0{\cdot}2 \times 10^{-8}$ A gives the upper limit of the shunt current and it can be concluded that when V_{post} was 20 mV, the maximum error in I_{post} was 3·2%. In contrast, similar calculations for the hyperpolarizing part of Text-fig. 13*d* show that, except for very small values of $-V_{post}$, large errors were attributable to shunting by the synapse (compare Text-fig. 10*c*, *d*). At $V_{post} = -20$ mV, up to 35% of the applied current entered the post-fibre by way of the junction. These large errors did not, however, affect the analysis of the synaptic rectifier described above; for in those calculations only the depolarizing and initial hyperpolarizing parts of the post-fibre curve were used.

The pre-fibre current–voltage curve was less affected by the nearness of the micro-electrodes to the synapse. Because of the lower 'input resistance' of the lateral giant axons, a smaller fraction of the applied current crossed the junction. Thus even for a pre-fibre depolarization of 25 mV, during which the resistance of the synapse was almost as low as for a hyperpolarization of the post-fibre of 20 mV, the error in I_{pre} was not greater than 6%. For small depolarizations and hyperpolarizations it was negligible; and these were the only parts of the pre-fibre curve used in constructing the characteristic curve of the synapse.

The rectifier in nerve-impulse transmission. The question now arises whether the above results can explain the transmission of the action potential. Are the synaptic currents that accompany a spike in the pre-fibre adequate to account entirely for the p.s.p.'s? The direction of current flow is correct, for the pre-fibre spike represents a large positive increase in V_{pre}; and as long as V_{pre} exceeds V_{post}, V_s and I_s are also positive ($V_s = V_{pre} - V_{post}$). In attempting to make a quantitative test of this question it has not been possible to apply directly the above analysis of the synaptic rectifier, for spikes and the experimental electrotonic pulses differed considerably in amplitude and time course. The largest electrotonic change in V_{pre} was only about 65% of the pre-fibre action potential. This precludes a direct comparison of the two situations, since the resistance of the synapse is different at different values of V_{pre}. The relatively short time course of the pre-fibre spikes also introduces a difficulty; for the spikes would be subject to additional attenuation, over that found for steady depolarizations, due to the capacitative properties of the post-fibre membrane. Another factor bringing about an increased attenuation of transients would be a delay in the change in synaptic resistance following a change in V_s (i.e. delayed rectification). The available results are, however,

insufficient to determine whether a significant delay in synaptic rectification was present. But despite these difficulties it seems likely from indirect evidence that the same mechanism accounts for transmission of electrotonic pulses and action potentials.

The two situations are compared in Table 2. The spikes were more attenuated than the catelectrotonic potentials in every experiment, despite their being larger and the fact that S decreases as V_{pre} increases. The mean difference between the two attenuation factors was about 40% and it seems probable that this difference would have been even greater if the electrotonic potentials had been larger. The greater attenuation of spikes was to be expected, if they were transmitted by the same mechanism as the steady potential changes, for the reasons given above.

TABLE 2. A comparison between the orthodromic attenuation factors for steady catelectrotonic potentials (α_c) and nerve impulses (α_s)

	Steady depolarizations			Spikes			
Expt.	V_{pre} (mV)	V_{post} (mV)	α_c	Spike (mV)	p.s.p. (mV)	α_s	α_s/α_c
1	60	13·5	4·5	100	18	5·6	1·25
2	45	15·9	2·8	80	20	4·0	1·43
3	30	6·7	4·5	72	12	6·0	1·34
4	20	9·5	2·1	70	24·5	2·9	1·38
5	35	9·3	3·8	80	16	5·0	1·33
6	30	10·0	3·0	78	20·7	3·8	1·27
7	50	22·5	2·2	80	28	2·9	1·32
8	50	26·5	1·9	80	30	2·7	1·42
9	45	11·3	4·0	90	13	6·9	1·73
10	55	10·0	5·5	85	9·8	8·7	1·58
Mean	42	13·5	3·4	81·5	19·2	4·9	1·41

In determining α_c, steady pulses of outward membrane current were applied to the pre-fibre while recording pre- and post-fibre membrane potentials (Text-fig. 12*a*, *b*). The maximum alteration in pre-fibre potential is given in the first column (V_{pre}), and the accompanying change in post-fibre potential (V_{post}) is shown in the second column. In the third column, $\alpha_c = V_{pre}/V_{post}$. The next three columns show the analagous findings for pre-fibre spikes and their accompanying p.s.p.'s, α_s being the quotient of spike divided by p.s.p. The ratio of these two attenuation factors is given in the last column.

The variability in α_c and α_s in Table 2 was considerable; but within any particular experiment the two factors tended to vary in the same way. The range of variation for α_s/α_c was only about one-eighth that for either of the attenuation factors by itself. A calculation of the coefficient of correlation between α_c and α_s for the ten pairs of values in Table 2 gave $r = 0{\cdot}95$, suggesting that the same variables determined the effectiveness of transmission in both cases. For the circuit of Text-fig. 11, in the orthodromic situation, $\alpha = 1 + S/R_{post}$, so that variations in either S or R_{post} would equally affect attenuation; and the question arises whether the high correlation between the two factors was due mainly to their dependence on R_{post}. The correlations of α_s with R_{post} and with S, were separately determined; for α_s and R_{post}, $r = -0{\cdot}11$

and for α_s and S, $r=0{\cdot}82$. Thus the high correlation between α_c and α_s is compatible with the synaptic resistance being the main variable controlling the size of the p.s.p.

DISCUSSION

The experiments described above provide very strong evidence for a type of 'electrical' transmission; that is, a situation in which the pre-fibre action potential, itself, is the electromotive force for the current of the p.s.p. The diverse transynaptic effects obtained by applying depolarizing or hyperpolarizing currents to pre- or post-fibre are simply explained by the synaptic-rectifier hypothesis, while mechanisms based upon the release of transmitter substances do not provide an acceptable alternative. For example, it is difficult to see how the experimentally produced transfer of hyperpolarizations from post- to pre-fibre could be explained in terms of a chemical transmitter mechanism. On the other hand, on an 'electrical' hypothesis this result follows quantitatively from the rectifier properties of the synapse as determined in an entirely different experimental situation, namely by orthodromic depolarizations.

The fact that transmission at the GMS's is usually strictly one-way, an antidromic spike giving rise to a negligible effect in the pre-fibre, is accounted for by the rectifier properties of the synapse. A spike in the post-fibre represents a large, positive increase in V_{post}, so that V_s becomes negative ($V_s=V_{pre}-V_{post}$) and the intensity of the synaptic current is very low (see Text-fig. 16). While it is clear that the rectifier ensures one-way transmission, the fact that the pre-fibre is larger than the post-fibre must also contribute to the 'asymmetry' of transmission. In the absence of synaptic rectification the ratio of the attenuation factors (α_0 and α_a) in the orthodromic and antidromic cases is given by,

$$\alpha_a/\alpha_0=\{(R_{pre}+S)/R_{pre}\}/\{(R_{post}+S)/R_{post}\}. \quad (1)$$

In a typical situation, in which $R_{post}/R_{pre}=5$ and taking $S=R_{post}$, $\alpha_a/\alpha_0=3$. This was approximately the value found for one of the six cases considered above in the section on antidromic nerve-impulse transmission, and in this case there was no apparent synaptic rectification. At the other five junctions, at which the rectifier was operating, α_a/α_0 was greater than fifty. It should be pointed out that while equation (1) is appropriate for steady potential changes at a non-rectifying synapse, it takes no account of differences in the membrane time constants of the two fibres. Nevertheless, this comparison gives a very rough measure of the importance of the rectifier in blocking antidromic effects. In its presence the pre-fibre potentials accompanying an antidromic spike in the post-fibre are negligible, but if the current–voltage characteristic for the synapse were linear, potential changes of the order of 10 mV (i.e. about one-third of the orthodromic p.s.p.) might be expected. Although it is

unlikely that one-to-one antidromic transmission would occur in this situation, rectification does prevent the transmission of appreciable local potential changes in the 'wrong' direction. The preceding discussion concerned synapses at which lateral giant axons were the pre-fibres. At the medial GMS's (i.e. between medial and motor giant fibres) the pre- and post-fibres are more nearly of equal size. In the absence of the synaptic rectifier, it seems likely that antidromic effects would be larger than at the lateral GMS's; but no experimental evidence on this point has been obtained.

An alternative way of discussing the functional significance of the rectifier is to consider it as a mechanism for providing a low synaptic resistance to current flow in the forward direction, rather than as a device for blocking antidromic effects. For example, in the experiment of Fig. 15 the resistance of the synapse was about $5{\cdot}5 \times 10^5\ \Omega$ when V_s was 25 mV ($S = V_s/I_s$). If the area of the 'synaptic membrane' is taken as 10^{-4} cm^2 (see Methods) then the resistance × unit area of this membrane was 55 Ω cm^2 at this value of 'membrane potential'. In the same experiment the resistance × unit area of the pre-fibre membrane, for a uniform depolarization of 25 mV, was found to be 390 Ω cm^2, using the method of Cole & Curtis (1941). Thus at this value of 'membrane' potential the resistance of the 'synaptic membrane' was about one-seventh that of a similar area of axon membrane.

Although the 'synaptic membrane' seems to be composed of contributions from the two axons, it behaves like a unit structure to the extent that the current traversing it appears to depend only on the p.d. across it. In the above model of the synapse (Figs. 10 and 11) it was assumed that there was no separation between the component membranes; or, if any existed, that the shunt resistance, R_e, between this space and extracellular fluid was high. This was the simplest model and the easiest to analyse. It must be noted, however, that R_e can be given relatively low values, approaching the order of R_{post}, without changing conditions seriously. For example, if R_e is given the same value as R_{post} and is considered to connect the centre of the synaptic resistance to the external fluid (and taking $R_{post}/R_{pre} = 4$), then for a given V_s the apparent synaptic current in the orthdromic situation would be about 20% less than that calculated for the antidromic. In several of the four-micro-electrode experiments, discrepancies of at least this size and direction were found. While the disparities were assumed to arise from errors due to spatial decrement of the electrotonic potentials, it is also possible that a finite value of R_e was a contributory factor. The presence of R_e would reduce the efficiency of transmission, but the effect could readily be compensated by a reduction in the synaptic-membrane resistance, S.

Studies of the structure of the GMS's of the crayfish (*Cambarus*) have been made histologically and with the electron microscope (Robertson, 1952, 1953, 1955) and also provide support for the idea that little separation may

exist between the components of the 'synaptic membrane'. Despite both pre- and post-fibres having Schwann-cell and connective-tissue sheaths, the membranes bounding the axoplasms come very close to one another at numerous places in the junctional region. The juxtaposition is brought about by short processes or tubular extensions of post-fibre membrane which penetrate the sheaths of both fibres. The ends of these processes spread out in the space between Schwann cell and pre-fibre axon-membrane, thus making patches in which the two fibre membranes are close together. One of these processes is shown in Pl. 1, a phase-contrast photomicrograph of a transverse section of *Astacus* abdominal nerve cord. The giant motor fibre, labelled 'post', is seen in oblique section crossing over the lateral giant pre-fibre. The arrow indicates a process, about 2–3 μ in diameter, extending from post- to pre-fibre; but the terminal expansion of the process cannot be seen. The section also includes the medial giant fibre of that side and three of the smaller motor axons which accompany the post-fibre in the third root. The disparity between the sizes of lateral and medial pre-fibres is greater than usual.

Electron micrographs show that the juxtaposition of the two fibre membranes can be a very close one. In Fig. 1 of Robertson (1955) the axoplasms of a medial giant pre-fibre and of a post-fibre process are shown separated by a structure which varies from about 150–300 Å in thickness, and which consists of the axon-membranes of the two fibres. Since the individual components of this double membrane are each about 75 Å thick (Robertson, personal communication) the space between them must vary in width from a negligible amount to about 150 Å. It is not known whether the negligible separation of the components, at places in the synaptic membrane, is an artifact.

The synapses in the stellate ganglion of the squid, between second- and third-order giant fibres, morphologically resemble the crayfish GMS's. They were the first example of this type of junction in which giant axons are synaptically connected by processes sent out from post- to pre-fibre (Young, 1939). Despite the anatomical resemblance the mechanism of transmission at the two synapses is apparently different. Bullock & Hagiwara (1957) and Hagiwara & Tasaki (1958) have concluded that transmission across the squid synapse is not brought about by local-circuit current crossing the junction, but by means of a special transmitter substance. Among other evidence supporting this conclusion was the presence of a long synaptic delay, so that the pre-fibre spike could be completed before the onset of the p.s.p. This is in contrast to the very short delays which have been observed at the crayfish GMS and which are compatible with the 'electrical' theory. The fact that the two types of synapse seem to differ in their mechanism of transmission, despite their anatomical similarity, suggests that any structural difference occurs at a finer level of organization. For example, one would like to know more exactly the extent of the space between pre- and post-fibre membranes at the two

junctions. For maximum efficiency, at an 'electrical' synapse, the separation would be negligible; but at a 'chemical' junction the space would have to have a relatively low resistance to the external medium. In his earlier studies, Robertson (1952, 1953) also made electron micrographs of the squid giant synapses and confirmed that processes from the post-fibre brought post-synaptic membrane in close apposition to pre-fibre membrane. With the techniques then available, however, it was not possible to determine accurately the size of this space and additional work on this point is needed.

It will be recalled that each post-fibre also makes synaptic connexion with the two medial giant axons (see Methods). Although in most of our experiments the lateral giant pre-fibres were used, in a few cases the GMS's between motor and medial giant axons have also been studied. These junctions have been found to resemble the lateral giant synapses, for electrotonic potentials traversed them but, again, only appreciably when the pre-fibre was depolarized or the post-fibre hyperpolarized. A complete analysis (as in Text-fig. 15) has not been made; but in experiments on five ipsilateral and one contralateral medial GMS's results analogous to those of Text-fig. 9 have been found. In addition, at one of the ipsilateral junctions, a second micro-electrode was inserted into the post-fibre and a curve similar to Text-fig. 13*b* was obtained.

The effects of various pharmacological agents on the GMS of *Cambarus* have been studied by Wiersma & Shalleck (1947, 1948; Schalleck & Wiersma, 1948). Nicotine and related compoounds were among the few substances which had an effect in relatively low concentrations. Facilitation of transmission usually occurred with 10^{-6} g/ml., inhibition with more concentrated solutions. We have made a few preliminary tests, recording the p.s.p. intracellularly, to see if these results could also be obtained with *Astacus*; but only small and variable effects have so far been observed, using nicotine concentrations up to 10^{-4} g/ml. There are a number of ways in which a drug might affect transmission. A reduction in the size of the pre-fibre spike, a lowering of the post-fibre membrane resistance, an increase in post-fibre threshold, or a hyperpolarization or large depolarization of the post-fibre, as well as a direct effect on the 'synaptic membrane', could all serve to bring the p.s.p. below firing level. In addition, nicotine might produce its action by altering the spontaneous activity at other synapses on the post-fibre (Furshpan & Potter, 1959). It is clear that further work is needed to determine the site of action of nicotine in *Cambarus* and to confirm its lack of effect in *Astacus*.

In most of our experiments, the post-fibres were considerably affected by the experimental procedure. Many of them failed to show all-or-nothing action potentials, but gave only graded, local responses to supraliminal depolarizations (e.g. Text-fig. 12*d*). While the absence of a conducted post-fibre spike prevented testing for antidromic impulse transmission, it does not seem to have affected the main results obtained with steady current pulses. In

those experiments (e.g. Text-fig. 7*a*) in which the post-fibre did conduct action potentials, the results were essentially the same as those obtained from less satisfactory preparations. Furthermore, the condition of the synapse could apparently vary independently of the condition of the post-fibre. For example, in the experiment of Text-figs. 12–16 the post-fibre gave only local, graded spikes yet the synapse appeared to work well. A pre-fibre spike (90 mV) gave rise to a potential change in the post-fibre greater than 40 mV. Since the membrane potential level at which an active response first appeared was about 30 mV, the post-synaptic potential change must have consisted partly of local response; and one-to-one transmission would presumably have taken place if the action potential mechanism had been operating properly.

The GMS's have several properties which result directly from the presence of the synaptic rectifier mechanism, but are also found at junctions with 'chemical' transmission. These properties cannot, therefore, be used to distinguish this type of 'electrical' synapse from the 'chemical' junctions: such are (1) the almost complete absence of pre-fibre potential change during an antidromic post-fibre spike; (2) an apparent decrease in post-fibre membrane resistance during transmission; (3) monophasic p.s.p.'s; and (4) a high degree of dependence of the size of the p.s.p. on the level of post-fibre membrane potential. The first point has already been discussed. The second, the apparent fall of R_{post} during a p.s.p., has not been demonstrated directly, but its presence is a necessary concomitant of the decrease in synaptic resistance. $S+R_{pre}$ is a shunt in parallel with R_{post} (see Text-fig. 11). Since S decreases to the order of R_{post} during transmission and R_{pre} is very small during pre-fibre activity, $S+R_{pre}$ will also be of the same order as R_{post}. The apparent value of R_{post} measured in the junctional region during transmission probably falls, therefore, to about one half of its resting level. The monophasic p.s.p.'s at the GMS come about because the pre-fibre spike, which provides the e.m.f., is monophasic. In this respect the GMS differs (i) from the situation of electrical interaction between adjacent axons in which the excitability changes in the 'post-fibre' are triphasic (Katz & Schmitt, 1940) and (ii) from the now discarded models for electrical transmission in which the p.s.p.'s were considered to be diphasic (e.g. Eccles, 1946). A more appropriate model for the GMS is a blocked nerve fibre in which the potential changes beyond the block are monophasic (Hodgkin, 1937). Concerning the fourth point, it has been observed in several experiments that the p.s.p. amplitude can be varied over a wide range by displacing post-fibre membrane potential. Depolarizations reduced the size of the p.s.p.'s while hyperpolarizations increased it. In one experiment the p.s.p., which was 17 mV when the steady level of post-fibre membrane potential was at the resting value ($V_{post}=0$), varied from 5 to 28 mV as V_{post} was altered over the range +37 to −40 mV. This effect results from the dependence of V_s and S on V_{post} ($V_s=V_{pre}-V_{post}$ and $S=f(V_s)$).

During post-fibre depolarizations, for example, V_s becomes less positive and, owing to the synaptic rectifier characteristic, S increases. Both factors thus cause a reduction in I_s ($=V_s/S$) and, therefore, in the p.s.p.'s. With this type of mechanism it would not be possible, however, to reverse the sign of the p.s.p. and in this respect the GMS differs from 'chemical' synapses (e.g. del Castillo & Katz, 1955; Burke & Ginsborg, 1956; also see Furshpan & Potter, 1959).

The above experiments have shown that pre-fibre depolarizations and post-fibre hyperpolarizations give rise to equal synaptic current provided the same p.d. across the junction is brought about. If the synapse behaves like a passive circuit element, this dependence of I_s on V_s should also hold when a given value of V_s is established at various absolute levels of the fibre membrane potentials. This has been tested in a few preliminary experiments, simultaneously changing V_{pre} and V_{post} by combined application of current to both fibres; and the expected relationship between I_s and V_s was found.

SUMMARY

1. The mechanism of impulse transmission has been studied at the giant motor synapses of the crayfish, by inserting one or two micro-electrodes into both pre- and post-synaptic axons. These fibres could be readily recognized by their distinctive physiological characteristics. The distance of the pre-fibre electrodes from the synapse was usually 10–20% of the characteristic length of that fibre. At least one of the post-fibre electrodes was usually in the immediate region of the junction.

2. With a recording electrode in each fibre it was found, during orthodromic nerve-impulse transmission, that the delay between the foot of the pre-fibre spike and the beginning of the p.s.p. was very small (usually about 0·1 msec).

3. An antidromic nerve impulse in the post-fibre gave rise to only a minute potential change in the pre-fibre (usually less than 0·5 mV).

4. Tests were made as to whether electrotonic potentials could cross the synapse, and it was found that even subthreshold depolarizations of the pre-fibre were accompanied by appreciable, but smaller, depolarizations of the post-fibre. Pre-fibre hyperpolarizations, however, gave rise to negligible changes in post-fibre potential. When the pulses of current were applied to the post-fibre, the results were apparently reversed; for now hyperpolarizations of the post-fibre gave rise to appreciable pre-fibre hyperpolarizations, whereas depolarizations were accompanied by only negligible transynaptic potential changes.

5. These seemingly diverse results could be explained by a simple hypothesis: electrotonic current readily flows across the junction, but the 'synaptic

membrane' is a rectifier allowing positive current to cross only in the direction from pre- to post-fibre.

6. In order to test this hypothesis, the current–voltage characteristic of the synaptic rectifier needed to account for the observed results was constructed. In fact, two such curves were made, one to account for depolarizations traversing the junction from pre- to post-fibre, and the other for hyperpolarizations crossing in the opposite direction. The two curves were found to be identical and the two situations were thus accounted for by the same mechanism, namely, the 'synaptic rectifier'. The results also showed that current flow across the synapse is determined simply by the p.d. across it (i.e. the difference between the internal potentials of pre- and post-fibre). Alternatively, 'chemical' mechanisms cannot adequately account for the transfer of hyperpolarizations from post- to pre-fibre.

7. The 'synaptic rectifier' is oriented in the right direction to allow local currents associated with a pre-fibre action potential to stimulate the post-fibre. It blocks oppositely directed currents, accompanying a post-fibre spike, and thus accounts for the absence of antidromic transmission. There is some evidence that the synaptic current that accompanies a pre-fibre spike is adequate to account for normal transmission.

8. The functional significance and structure of the synapse was discussed. As well as blocking antidromic effects, the 'synaptic rectifier' provides a low resistance for transmission in the orthodromic direction. In one case the resistance of the 'synaptic membrane' was estimated to be about one-seventh that of a comparable area of pre-fibre membrane with the same p.d. across it.

It is a pleasure to thank Professor B. Katz for suggesting the crayfish synapses to us as an object of study and for continual advice and encouragement during the course of the work. We also wish to acknowledge our debt to Professor S. W. Kuffler, Dr B. Ginsborg, and Dr J. del Castillo for their helpful suggestions and comments; and to thank J. L. Parkinson, Audrey M. Paintin and K. S. Copeland for frequent assistance. Financial support was received from the National Science Foundation and the U.S. Public Health Service.

REFERENCES

BULLOCK, T. H. & HAGIWARA, S. (1957). Intracellular recording from the giant synapse of the squid. *J. gen. Physiol.* **20**, 565–578.

BURKE, W. & GINSBORG, B. L. (1956). The action of the neuromuscular transmitter on the slow fibre membrane. *J. Physiol.* **132**, 599–610.

COLE, K. S. & CURTIS, H. J. (1941). Membrane potential of the squid giant axon during current flow. *J. gen. Physiol.* **24**, 551–563.

DEL CASTILLO, J. & KATZ, B. (1954). Changes in end-plate activity produced by pre-synaptic polarization. *J. Physiol.* **124**, 586–604.

DEL CASTILLO, J. & KATZ, B. (1955). Local activity at a depolarized nerve-muscle junction. *J. Physiol.* **128**, 396–411.

DEL CASTILLO, J. & KATZ, B. (1956). Biophysical aspects of neuro-muscular transmission. *Progr. Biophys.* **6**, 121–170.

ECCLES, J. C. (1946). An electrical hypothesis of synaptic and neuro-muscular transmission. *Ann. N.Y. Acad. Sci.* **47**, 429–455.

ECCLES, J. C. (1957). *The Physiology of Nerve Cells.* Baltimore: Johns Hopkins.

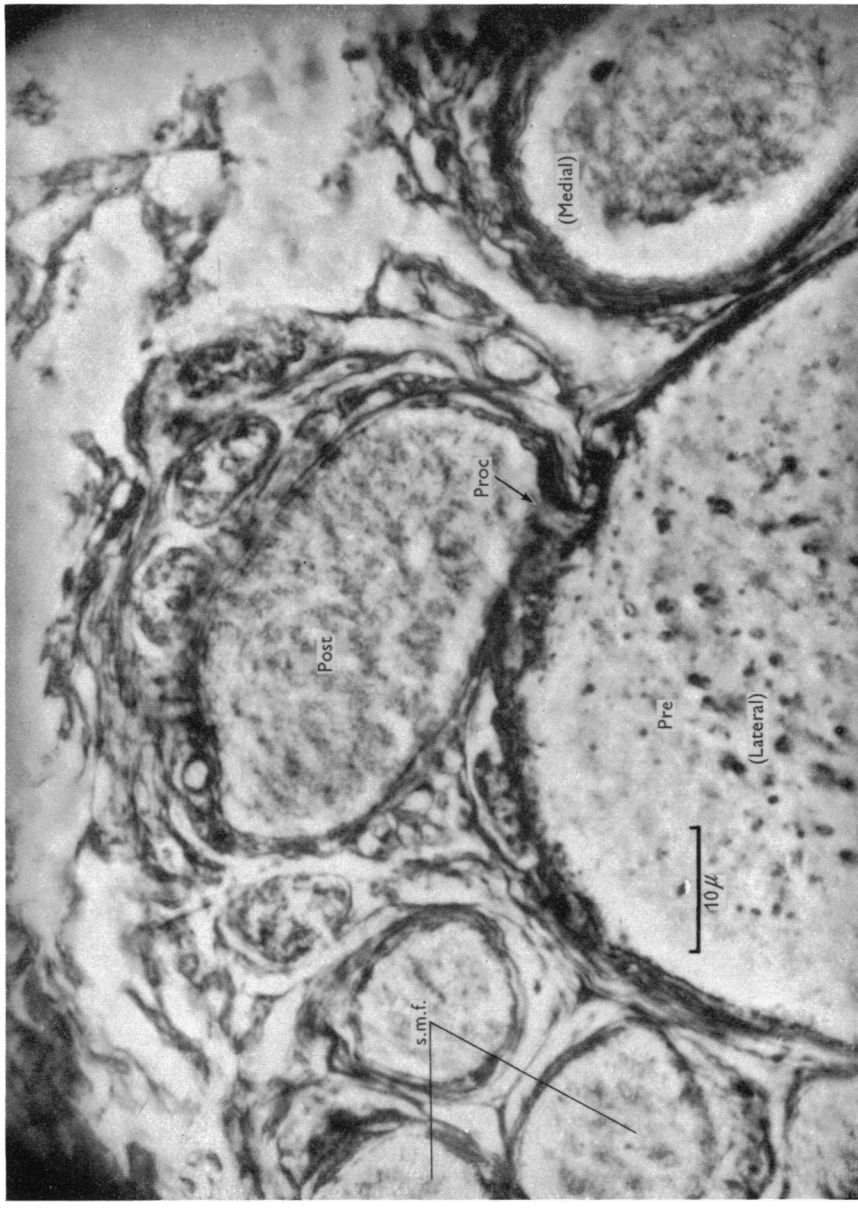

(*Facing p.* 325)

FATT, P. (1954). Biophysics of junctional transmission. *Physiol. Rev.* **34**, 674–710.

FATT, P. & KATZ, B. (1951). An analysis of the end-plate potential recorded with an intracellular electrode. *J. Physiol.* **115**, 320–370.

FURSHPAN, E. J. & POTTER, D. D. (1957). Mechanism of nerve-impulse transmission at a crayfish synapse. *Nature, Lond.*, **180**, 342–343.

FURSHPAN, E. J. & POTTER, D. D. (1959). Slow post-synaptic potentials recorded from the giant motor fibre of the crayfish. *J. Physiol.* **145**, 326–335.

GRUNDFEST, H. (1957). The mechanisms of discharge of the electric organs in relation to general and comparative physiology. *Progr. Biophys.* **7**, 1–85.

HAGIWARA, S. & TASAKI, I. (1958). A study of the mechanism of impulse transmission across the giant synapse of the squid. *J. Physiol.* **143**, 114–137.

HARDY, W. B. (1894). On some histological features and physiological properties of the post-oesophageal nerve cord of the Crustacea. *Phil. Trans.* B, Part I. **185**, 83–117.

HODGKIN, A. L. (1937). Evidence for electrical transmission in nerve. Part I. *J. Physiol.* **90**, 183–210.

JOHNSON, G. E. (1924). Giant nerve fibres in crustaceans with special reference to *Cambarus* and *Palaemonetes*. *J. comp. Neurol.* **36**, 323–373.

KAO, C. Y. & GRUNDFEST, H. (1956). Conductile and integrative functions of crayfish giant axons. *Fed. Proc.* **15**, 104.

KATZ, B. & SCHMITT, O. H. (1940). Electrical interaction between two adjacent nerve fibres. *J. Physiol.* **97**, 471–488.

NASTUK, W. L. & HODGKIN, A. L. (1950). The electrical activity of single muscle fibres. *J. cell. comp. Physiol.* **35**, 39–73.

ROBERTSON, J. D. (1952). Ultrastructure of an invertebrate synapse. *Thesis*, Massachusetts Institute of Technology: Cambridge, Mass., U.S.A.

ROBERTSON, J. D. (1953). Ultrastructure of two invertebrate synapses. *Proc. Soc. exp. Biol., N.Y.*, **82**, 219–223.

ROBERTSON, J. D. (1955). Recent electron microscope observations on the ultrastructure of the crayfish median-to-motor giant synapse. *Exp. Cell Res.* **8**, 226–229.

SCHALLECK, W. & WIERSMA, C. A. G. (1948). The influence of various drugs on a crustacean synapse. *J. cell. comp. Physiol.* **31**, 35–47.

STOUGH, H. B. (1926). Giant nerve fibres of the earthworm. *J. comp. Neurol.* **40**, 409–443.

VAN HARREVELD, A. (1936). A physiological solution for fresh-water crustaceans. *Proc. Soc. exp. Biol., N.Y.*, **34**, 428–432.

VOM RATH, O. (1895). Zur Conservirungstechnik. *Anat. Anzeig.* **11**, 280–288.

WIERSMA, C. A. G. (1947). Giant nerve fibre system of the crayfish. A contribution to comparative physiology of synapse. *J. Neurophysiol.* **10**, 23–38.

WIERSMA, C. A. G. & SCHALLECK, W. (1947). Potentials from motor roots of the crustacean central nervous system. *J. Neurophysiol.* **10**, 323–329.

WIERSMA, C. A. G. & SCHALLECK, W. (1948). Influence of drugs on response of a crustacean synapse to pre-ganglionic stimulation. *J. Neurophysiol.* **11**, 491–496.

YOUNG, J. Z. (1939). Fused neurons and synaptic contacts in the giant nerve fibres of cephalopods. *Phil. Trans.* **229**, 465–503.

EXPLANATION OF PLATE

A transverse section of crayfish nerve cord through the region of a lateral GMS. Phase-contrast. The arrow (proc) indicates a post-fibre process which extends to the lateral giant pre-fibre. The medial giant fibre (medial) of the same side is seen on the right, with three of the smaller fibres of the third root (s.m.f.) on the left. Modified vom Rath's (1895) fixative.